Natural Hazards
https://doi.org/10.1007/s11069-023-05937-8

ORIGINAL PAPER

Methodology to incorporate seismic damage and debris to evaluate strategies to reduce life safety risk for multi-hazard earthquake and tsunami

Mehrshad Amini[1] · **Dylan R. Sanderson**[1] · **Daniel T. Cox**[1] · **Andre R. Barbosa**[1] · **Nathanael Rosenheim**[2]

Received: 15 July 2022 / Accepted: 22 March 2023

Abstract
This paper presents a methodology to evaluate life safety risk of coastal communities vulnerable to seismic and tsunami hazards. The work explicitly incorporates two important aspects in tsunami evacuation modeling: (1) the effect of earthquake-induced damage to buildings on building egress time, (2) the effect of earthquake-induced debris on horizontal evacuation time. The city of Seaside, Oregon, is selected as a testbed community. The hazard is based on a megathrust earthquake and tsunami from the Cascadia Subduction Zone that was defined in a previous study. The built environment consists of buildings and the transportation network for the city. Fragility analysis is used to estimate the seismic damage to buildings and resulting debris that covers portions of the road network. The horizontal evacuation time is determined based on the shortest path to shelters, including the increased travel time due to the earthquake-generated debris. The effects of different mitigation strategies are quantified. Results indicate the fatality and life safety risk of a near-field tsunami increases by 4.2–8.3 times when the effects of building egress and earthquake-induced debris are considered. The choice of population layer affects the life safety risk and thus the maximum risk is obtained when daytime populations are considered. Use of mitigation strategies result in a significant decrease in the number of fatalities. For hazards with recurrence intervals larger than 500- to 1000-years, the seismic retrofit is comparable to vertical evacuation and an effective strategy in reducing fatalities and associated risks. Implementing all mitigation strategies reduces the life safety risk by 90%.

Keywords Tsunami evacuation · Building egress · Earthquake-induced debris · Life safety risk · Vertical evacuation · Disaster mitigation · Risk reduction

✉ Mehrshad Amini
mehrshad.amini@oregonstate.edu

✉ Dylan R. Sanderson
sanderdy@oregonstate.edu

✉ Andre R. Barbosa
Andre.Barbosa@oregonstate.edu

Extended author information available on the last page of the article

Published online: 09 May 2023

1 Introduction

1.1 Background

Tsunamis are devastating natural disasters primarily triggered by major earthquakes, which not only impose direct and indirect economic losses, but also result in a remarkable loss of life. Tsunamis can be low-probability and high-consequence events that have greatly threatened many coastal communities throughout the world (Ritchie and Roser 2014). For example, the 2010 Chile tsunami caused about $30 million in economic losses and nearly 645 deaths (Fritz et al. 2011; Salazar and Marcia 2011). The 2004 Indian Ocean and the 2011 East Japan tsunamis are estimated to have caused a loss of life of over 225,000 and 24,000 people, respectively (Mimura et al. 2011; Okal 2015; Shuto and Fujima 2009; Suppasri et al. 2013). Off the western coast of the United States and Canada, the Cascadia Subduction Zone (CSZ) is a major source that has the potential to generate strong ground shaking and tsunami inundation in many coastal communities of the Pacific Northwest and Northern California regions (Goldfinger et al. 2012; Heaton and Hartzell 1987; Wood 2007; Wood et al. 2013) with the probability of occurrence of earthquake ranging from 10 to 14% in the next 50 years (Petersen et al. 2002; Witter et al. 2013). In addition, the risk is expected to increase in the future due to the population and urban growth in coastal areas (Cremen et al. 2022; Neumann et al. 2015). For communities affected by near-field events that have both strong seismic ground motion and subsequent tsunami inundation, the number of casualties can be still devastating due to uncertainties in both tsunami inundation and human behavior, particularly during the evacuation process. Therefore, understanding potential challenges in the tsunami evacuation plan and corresponding mitigation strategies can significantly reduce the number casualties in coastal communities.

Unlike a far-field tsunami, a near-field tsunami is likely to reach the onshore within 20–40 min after the initial earthquake, which can impose a greater risk and threaten the life safety in coastal communities (Henry et al. 2017; Katada et al. 2006). Due to short arrival time of the near-field tsunami, a rapid evacuation that is more likely to be on foot can considerably increase the probability of surviving (Fraser et al. 2014; Katada et al. 2006). Due to the pressing need to mitigate the life safety risk, several researchers and state agencies have focused their studies on the impact of near-field tsunamis on life safety to develop effective tsunami evacuation plans that minimize the casualties (e.g., Makinoshima et al. 2020; Priest et al. 2016; Wilson and Miller 2014). While the findings have revealed that an efficient evacuation plan is essential to minimize casualties, there remains a lack of sufficient understanding of the life safety risk for coastal communities vulnerable to seismic and tsunami events (Mas et al. 2015; Wang et al. 2016; Xie and Muraki 2017) due to lack of integration of impacts of debris due to the damage infrastructure and buildings on the evacuation modeling (Castro et al. 2019; Kameshwar et al. 2021; Mostafizi et al. 2017).

1.2 Study scope

This paper presents a methodology to simulate tsunami evacuation of people, estimate casualties, and ultimately assess the life safety risk due to seismic and subsequent tsunami hazards at the community level. The city of Seaside, Oregon, vulnerable to the seismic and near-field tsunami due to the CSZ, is selected as an example community to illustrate the application of the methodology. The methodology explicitly incorporates two important

aspects in the tsunami evacuation modeling: (1) the effect of earthquake-induced damage to buildings on building egress time, (2) the effect of earthquake-induced debris on horizontal evacuation time. The population layers account for residents, workers that commute to the city, and tourists at the parcel level. The casualty rates are calculated for each parcel considering different community preparedness levels as well as daytime and nighttime population layers. The horizontal evacuation time is determined based on the shortest path to safety, in which it has been assumed that all evacuees will follow evacuation signs. In addition, the behavioral interaction among evacuees is not considered since it is computationally expensive, particularly when a large population is considered. The results are compared in terms of the number of casualties and associated risks to quantify the effect of different mitigation strategies, namely improving tsunami readiness, using vertical evacuation shelters, and seismic retrofitting methods on the life safety. Finally, a sensitivity analysis is performed to evaluate the effect of different levels of tsunami preparedness and debris models on the tsunami casualty results. The open-source Interdependent Networked Community Resilience Modeling Environment (IN-CORE) developed by Center for Risk-Based Community Resilience Planning is utilized for the building damage analyses in this study. All other models were implemented in python on a Jupyter notebook.

The paper is organized as follows. In Sect. 2, the literature review about earthquake and tsunami evacuation models are presented. In Sect. 3, the proposed methodology is presented. In Sect. 4, the proposed methodology is applied to the testbed community. In Sect. 5, simulation inputs depending on the selected testbed are presented. Section 6 provides the results and comparisons, including earthquake and tsunami casualties, mitigation strategies, and the sensitivity analysis. Section 7 presents the discussion of the results, limitations, and future research suggestions. Finally, in Sect. 8, conclusions are presented.

2 Literature review

In this section we review casualty models for both earthquakes and tsunamis. Observations from earthquake events demonstrate that direct seismic damage to the infrastructure such as buildings is responsible for almost 75% of casualties (Rahman 2018; Zuccaro and Cacace 2011). There are primarily two types of earthquake casualty models (Chaoxu et al. 2022). In this first model, damage to buildings is not considered, and casualties are estimated based on earthquake parameters such as the magnitude and intensity. Based on various earthquake parameters, there are different models (e.g., Badal et al. 2005; Christoskov and Samardjieva 1984; Liu and Lin 2012), of which the US Geology Survey (USGS) is the most well-known model. In the second model, casualties are estimated based on different levels of damage to buildings and corresponding casualty rates (e.g., Furukawa et al. 2010; Ma and Xie 2000; Urrutia et al. 2014). In this regard, HAZUS earthquake casualty model has been extensively adopted to assess the earthquake casualty in vulnerable communities (e.g., Levi et al. 2015; Nastev and Todorov 2013; Shapira et al. 2018). Apart from that, historical seismic data has been utilized to validate casualty models (e.g., Aguirre et al. 2018; Remo and Pinter 2012; Rozelle 2018). It should be noted that although earthquake casualty models do not include human interaction at the same level of complexity as tsunami casualty models, earthquake evacuation and associated human interactions such as grouping behavior and information sharing remains critical to life safety (Bernardini et al. 2019; Gu et al. 2016; Spence and Scawthorn 2011; Zhu et al. 2020).

Early studies about the tsunami evacuation have been carried out in Japan due to its extensive experience with tsunamis, and then later expanded to other vulnerable communities (Pishief 2007; Shuto and Fujima 2009). Tsunami evacuation models are mainly classified into macroscopic or microscopic models (e.g., Hamacher and Tjandra 2002; Pidd et al. 1996). Modeling is straightforward and computationally efficient in macroscopic models that include static and dynamic networks (e.g., least-cost distance, shortest distance, and quickest flow models); however, these models are not able to fully describe the decision-making behavior and interaction between evacuees (Fraser et al. 2014; Lammel 2011; Muhammad et al. 2017; Priest et al. 2016; Wood and Schmidtlein 2012). On the other hand, microscopic models, such as agent-based models (ABM) integrated with network analyses can simulate the interaction between evacuees but require expensive computational resources, particularly when large populations and their temporal (daily and/or seasonal) fluctuations are considered (Macal and North 2010; Na and Banerjee 2019; Wang et al. 2016; Wang and Jia 2021; Wijerathne et al. 2013). Makinoshima et al. (2020) conducted a literature review to better understand the evacuation behavior in tsunamis. The study demonstrated that evacuees' behavior during the tsunami evacuation can be categorized into four stages, namely receiving notification, risk recognition, response activity, and evacuation movement. Therefore, understanding human behavior such as evacuees' cognitive, emotional behaviors, or levels of stress is critical, and can significantly affect the decision-making process during the evacuation (e.g., Charnkol and Tanaboriboon 2006; Mas et al. 2015; Takabatake et al. 2017). For example, Buylova et al. (2020) performed a household survey to realistically evaluate the effects of socio-environmental and demographic variables on tsunami risk recognition. Surprisingly, the outcomes indicated that experiencing past extreme events does not necessarily result in a higher likelihood of having immediate evacuation behavior since those experiences have various levels of impact on behavioral responses depending on several factors such as the time of the event, intensity and the extent of damage, and the level of casualty experienced by residents. Although several studies have shown that neglecting the evacuees decision-making behavior underestimates the evacuation time (Lammel 2011; Mas et al. 2012; Muhammad et al. 2021; Wang et al. 2016), the ABM requires critical inputs to fully consider evacuee's behavior resulting in several levels of complexity, particularly for emergency planners who often require information for a variety of potential events (Mls et al. 2022). Therefore, given the scope of this paper, the literature review mainly focuses on macroscopic models for the near-field tsunami evacuation.

Sugimoto et al. (2003) assessed the effect of early evacuation on the number of casualties in coastal regions of Shikoku Island, Japan. They concluded that early evacuation significantly reduces the number casualties. Katada et al. (2006) developed an integrated GIS-based tsunami evacuation model to systematicity evaluate the vulnerability of coastal communities. Freire et al. (2013) conducted a tsunami risk assessment based on the cost-weighted distance model to evaluate the effect of daytime and nighttime populations on tsunami evacuation modeling in the Lisbon Metropolitan Area. The results showed the population at risk can significantly increase from nighttime to daytime populations. Fraser et al. (2014) developed a tsunami evacuation framework based on a hypothetical near-field tsunami scenario utilizing the least-cost distance model to evaluate the vulnerability of coastal communities in Napier City, New Zealand. The results highlighted the significance of considering the uncertainty in population exposure characteristics such as evacuation preparation time and pedestrian walking speed. Wood and Schmidtlein (2012) assessed the sensitivity of the least-cost distance model to various input variables for pedestrian tsunami evacuation in Long Beach Peninsula, Washington. The results showed that several factors

can affect the evacuation travel time, including the anisotropic path assumption, land-cover resolution, and initial walking speeds. Wood and Schmidtlein (2013) conducted a vulnerability assessment to understand how variations in population exposure to a given tsunami can affect the pedestrian travel time. They focused on multiple coastal communities in Grays Harbor and Pacific Counties, WA, which are threatened by CSZ near-field tsunamis. The results demonstrated that communities face a wide range of vulnerabilities so that people in several communities are unable to successfully evacuate on foot due to short tsunami arrival time and large distances to safety zones. Similar studies have been carried out for multiple coastal communities in the Northern California region (Wood et al. 2017, 2020a). Frucht et al. (2021) developed a tsunami risk assessment based on a worst-case scenario for a vulnerable community in Haifa, Israel. They utilized the HAZUS Tsunami Model to estimate the casualty losses considering the resident population with different preparedness levels, where the transportation mode was only horizontal evacuation on foot. They concluded that increasing the community preparedness level and seismic retrofitting of existing structures are two main effective mitigation strategies, which can significantly decrease the casualty. In this regard, Bernardini and Ferreira (2022) showed that implementing a targeted seismic retrofitting plan for vulnerable historical buildings in urban regions is an effective mitigation strategy to reduce the building damage, facilitate the evacuation process, and improve the community's safety. Recently Wood et al. (2020b) incorporated a probabilistic tsunami hazard model in the tsunami evacuation model to understand the effect of uncertainties in hazards on evacuation variables such as wave-arrival time, inundated lands, and ultimately life safety. The results indicated that given the pedestrian evacuation modeling, increasing the tsunami recurrence interval results in a significant increase in the number of parcels with insufficient evacuation time.

As mentioned earlier, since the CSZ is a major source of the earthquake and near-field tsunami, several studies have been carried out to assess life safety for vulnerable coastal communities, particularly the city of Seaside, Oregon, located in the vicinity of the CSZ that has the highest vulnerability to tsunami hazards among Oregon coastal communities (Priest et al. 2015; Wood 2007). Priest et al. (2016) utilized the worst-case scenario for tsunami hazards along with least-cost distance model to evaluate the pedestrian evacuation for tsunamis and its potential challenges. The results indicated that the pedestrian evacuation in Seaside strongly depends on the functionality of bridges that are already vulnerable to seismic damage. Wang et al. (2016) developed an ABM framework to investigate the effect of various decision-making variables on the tsunami evacuation in Seaside. They considered a peak summer weekend as a worse-case scenario with total 2500 evacuees impacted by a scenario-based tsunami inundation with the 500-year recurrence interval. The results of study lead to the conclusion that the fatality rate is significantly sensitive to different factors, including the mode of transportation (walking versus car), departure time (immediate versus delayed evacuation), evacuation speed (slow walk versus fast walk), choice of the evacuation route, and the evacuation mode (horizontal versus vertical shelters). Capozzo et al. (2019) implemented the HAZUS methodology to assess direct losses, including the casualty for Seaside with a population layer of 6500 people due to 1000-year seismic and tsunami recurrence intervals. The results indicated that the joint seismic and tsunami hazard dramatically increases the number of fatalities mainly due to seismic damage to bridges, which can adversely affect the tsunami evacuation. One step further, Mostafizi et al. (2017) developed an ABM framework to assess the network vulnerability and identify critical links during the tsunami evacuation in Seaside. They concluded that alternative approaches to allocate resources for bridge retrofitting can significantly affect life safety outcomes. Furthermore, Mostafizi et al. (2019) extended the framework to evaluate the

vertical evacuation strategies for a scenario-based near-field tsunami in Seaside. The results indicated that while the logical location of the vertical shelter is at the city center with the high density of population, the fatality rate is significantly sensitive to other factors such as walking speed, preparation time, and the percentage of people who intend to evacuate using the vertical shelter. Given the high vulnerability of Seaside, although several studies have been performed to estimate seismic damage to the infrastructure (e.g., Park et al. 2017b; Sanderson et al. 2021; Wiebe and Cox 2014) and associated debris (Kameshwar et al. 2021; Park and Cox 2019), additional efforts are needed to consider the effect of such damage and associated debris on the tsunami evacuation modeling.

The above literature review has identified several research gaps, particularly in assessing the earthquake and tsunami life safety within coastal communities. First, to the authors' knowledge, there is no study investigating the impacts of earthquake on the tsunami evacuation, including the earthquake-induced damage to buildings on building egress time and associated debris on horizontal evacuation time. Second, most studies reviewed here adopted a deterministic approach in their earthquake and tsunami hazard characterization, focusing on simulations considering historical or hypothetical worst-case scenarios, which do not lend themselves to compute the life safety risk, which incorporates both the probability of occurrence of the hazards and their consequences. Third, most studies to date have focused on the census derived population characteristics; thus, resident, employee, and tourist populations as well as their daytime and nighttime variations have not been considered. Therefore, this paper proposes a methodology to address these research gaps and assess the life safety risk due to earthquake and tsunami hazards at the community scale. The results could assist stakeholders, decision makers, and urban planners to better understand the tsunami evacuation plan and estimate the associated life safety risk.

3 Methodology

Figure 1 shows the overall methodology utilized in this study to evaluate life safety for near-field earthquakes and tsunamis, and to investigate various mitigation strategies. The methodology is adapted based on the decision-support framework proposed by Kameshwar et al. (2019) for the community resilience assessment. As shown in Fig. 1, the first component, "decision support options" proposes several decision criteria, namely hazards and severity, infrastructure systems, social systems, resources, ex-ante strategies (mitigation), and ex-post (response) that can be adopted by stakeholders, decision makers, and urban planners. The first step in decision and support options is to identify hazards and severity that threaten the community (Fig. 1, Step 1). As the recurrence interval and severity of the hazard increases, the annual probability of occurrence decreases. Probabilistic seismic and tsunami hazards are required to conduct risk assessment, estimate the number of casualties, and associated risks. The second step is to select the infrastructure systems that are important to the community and have considerable impacts on selected resilience metrics. The third step entails identifying the social system, in this example, the population that is at risk due to earthquake and tsunami hazards. Finally, communities can evaluate different mitigation strategies and decide to implement the selected strategy based on resilience metrics such as life safety and associated risks. The second component, "hazard description" includes probabilistic seismic and tsunami hazards for several recurrence intervals. These hazards are utilized as inputs for the probabilistic simulations. The third component, "built environment" includes data and information about infrastructure systems, such as

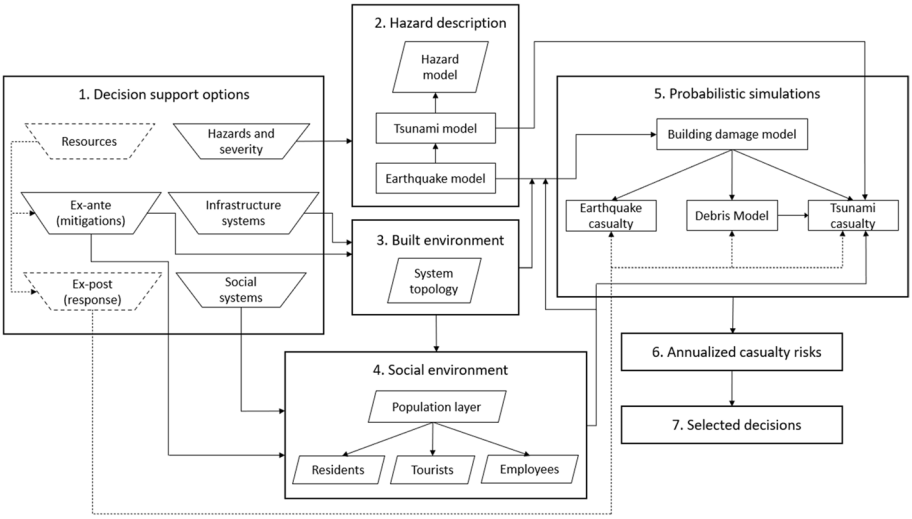

Fig. 1 Proposed methodology for the life safety risk assessment of near-field earthquake and tsunami

buildings, the transportation network (roadways and bridges), as well as other lifeline systems such as water, power, gas, and telecommunication. For example, building characteristics such as construction material, design level (e.g., pre-code, low-code, moderate-code, and high-code), year of construction, and number of stories can be estimated using various datasets and methods, including tax lot data, field survey, and Google Street View. In addition, mitigation strategies such as using a vertical evacuation shelter can directly impact the built environment. The built environment is utilized as one of the inputs that directly inform the social environment.

The fourth component, "social environment" consists of population layers, including residents, employees, and tourists with different spatial and temporal distributions (e.g., daytime versus nighttime). The resident population can be estimated based on the US Census. Since the US Census data provides demographic characteristics at the block level, a probabilistic method is needed to inform housing unit characteristics at the parcel level (e.g., Rosenheim et al. 2019). The employee population can be estimated based on different resources, such as the Data Axle USA Database (2020), which determines the number of employees for all business based on North American Industry Classification System (NAICS) codes at the parcel level. Unlike resident and employee populations, it is more challenging to estimate the tourist population due to limited resources. For example, the temporal fluctuation of visitors for daytime and nighttime population is essential to accurately evaluate the life safety risk for communities that attract a large number of tourists. In addition, certain allocation strategies are required to develop the high-resolution tourist population layer for daytime and nighttime. For example, for the daytime population, tourists need to be allocated in hotels, near the beach, and downtown areas. Therefore, given that methods for developing the tourist population need to be tailored to the selected community, details of the procedure for the testbed are presented in Sect. 5.4. Social environment.

The fifth component, "probabilistic simulation" consists of four main modules, namely building damage model, debris model, earthquake and tsunami casualty models.

The damage model estimates ground shaking-induced damage to buildings, through the application of appropriate structural and non-structural fragility curves (Attary et al. 2016, 2017, 2021; Alam et al. 2018). The debris model estimates the earthquake-induce debris due to both structural and non-structural damage to buildings. The earthquake casualty model is based on the HAZUS methodology, which employs the outputs from earthquake-induced damage to buildings along with indoor/outdoor casualty rates to estimate the total casualty (Federal Emergency Management Agency 2015). The model excludes casualties due to other factors such as heart attack, car accidents, fire, and post-earthquake activities. The casualty is estimated based on four severity levels of injuries, namely light injuries (*Severity 1*), hospitalized injuries (*Severity 2*), life threatening injuries (*Severity 3*), and deaths (*Severity 4*). Given the severity level, the casualty is calculated from two inputs, including damage state probabilities and associated indoor/outdoor casualty rates. The direct physical damage is determined using HAZUS seismic fragility curves representing the probability of exceeding different damage states for a given hazard intensity (Federal Emergency Management Agency 2015). Similarly, casualty rates are assigned based on severity levels, building types, and damage states. Additional details about the earthquake casualty model are provided in the HAZUS earthquake technical manual (Federal Emergency Management Agency 2015).

The tsunami casualty model was initially adopted from the HAZUS methodology (Federal Emergency Management Agency 2013), but then was extended to explicitly incorporates: (1) the effect of earthquake-induced damage to buildings on building egress time, (2) the effect of earthquake-induced debris on horizontal evacuation time. The HAZUS tsunami casualty model estimates the number of casualties (fatalities and injuries) due to only tsunami hazards, in which fatality rates are determined based on several parameters, including hazards, warning time, preparation time, travel time, and fatality boundary. The hazard includes information such as maximum inundation, tsunami arrival time, and maximum runup time. The preparation time is determined based on the level of community preparedness (Good, Poor, and Fair) depending on factors such as shore-protection structures, emergency loudspeakers, evacuation signs, and the education level for tsunami awareness (Federal Emergency Management Agency 2013). According to previous studies, the preparation time for tourists is more likely to be less than residents (Carlos-Arce et al. 2017; Charnkol and Tanaboriboon 2006; Takabatake et al. 2018). Regarding fatalities, the HAZUS model distinguishes between travel time to safety (regions with no inundation) and travel time to partially safety (regions where the inundation depth is less than or equal to 2 m). The travel time is calculated based on the macroscopic model and shortest distance to tsunami shelters using the transportation network and the selected evacuee speed. Therefore, as mentioned earlier, interactions among evacuees such as social and psychological factors are not considered here (e.g., Bernardini et al. 2019; Makinoshima et al. 2020). The model assumes that there is a 50% chance of fatality and 50% of injury for the partially safety regions. The fatality rate increases to 99%, and the injury rate decreases to 1% where the inundation is greater than 2 m. Additional details on the tsunami casualty model are provided in the HAZUS tsunami technical manual (Federal Emergency Management Agency 2013). It should be mentioned that while selecting the macroscopic model based on the shortest distance to tsunami shelters can negatively affect the outcomes (e.g., underestimating the travel time), it is computationally efficient, and given the scope of this study, the model can provide valuable insights about the tsunami life safety, particularly to better understand the effect of earthquake damage and the resulting debris on the tsunami evacuation modeling.

To incorporate building egress time in the model, the HAZUS model was initially adopted as a baseline to evaluate the life safety risk due to tsunami hazards. The critical time (T_{crit}) represents the time difference between the available time and the evacuation time to evacuate at the parcel level. Therefore, T_{crit} is calculated as:

$$T_{\text{crit}} = T_{\text{available}} - T_{\text{evacuation}} \tag{1}$$

$$T_{\text{available}} = T_{\text{max}} - T_{w} \tag{2}$$

$$T_{\text{evacuation}} = T_{\text{prep}} + T_{\text{travel}} + T_{\text{be}} \tag{3}$$

where T_{max} = maximum runup time; T_{w} = time to issue warning; T_{prep} = estimated preparation time; T_{travel} = travel time to safety; and T_{be} = building egress time. The variable T_{be} was added to the baseline model to account for the effect of earthquake-induced damage on building egress time. Liu et al. (2016) developed an agent-based model to study the effect of building damage due to the earthquake ground shaking on human evacuation behavior during the evacuation. As a result, building egress time for each building type (normal and overcrowded buildings) and damage scenario was estimated based on selected probability distributions. Note that, given the agent-based model used by Liu et al. (2016), the crowding effects have been originally considered in the estimation of building egress time, but no interaction among evacuees is considered in this study. The building egress time is assigned based on the occupancy type, building elevation, and damage level and does not explicitly consider the number of occupants (no crowding effect). The horizontal evacuation along the streets for traveling to the shelters does not consider the number of occupants and their interactions since the density is low, and the tsunami evacuation is only considered on foot.

To incorporate the effect of seismic debris in the model, the reduction coefficients affecting the walking speed were calculated from debris generated from damaged buildings. The debris weight (in tons) generated from each building due to the earthquake was calculated based on the HAZUS earthquake manual. According to this model, the total debris weight stems from both structural and non-structural damage for various building types, which results in both heavy debris (steel and reinforced concrete members) and light debris (brick, wood, and other materials). As the next step, a simplified model proposed by Argyroudis et al. (2015) was adopted to estimate the geometry of debris resulted from a damaged building. A similar approach was employed by Castro et al. (2019) to simulate the impact of earthquake-induced debris on the horizontal tsunami evacuation time. Figure 2 shows the simplified model with associated parameters to estimate the debris width (W_d), which is given by:

$$W_d = \sqrt{W^2 + \frac{2k_v WH}{\tan\theta}} - W \tag{4}$$

with $k_v = (WH_d + 0.5W_dH_d)/(WH)$, and where H and W are height and width of the undamaged building, respectively; k_v is the ratio of the volume of damaged building to the volume of undamaged building, H_d is the debris height, and θ is the angle of collapsed debris. As shown in Fig. 2, the undamaged and damaged buildings are depicted in solid and dashed lines, respectively. In the model, it is assumed that the debris volume will resemble a triangular prism with a larger height next to the building. Given the building height and width, the values of k_v and θ were considered as random variables, which resulted in a certain level of uncertainty in the value of the debris width (W_d). Finally, pieces of debris were

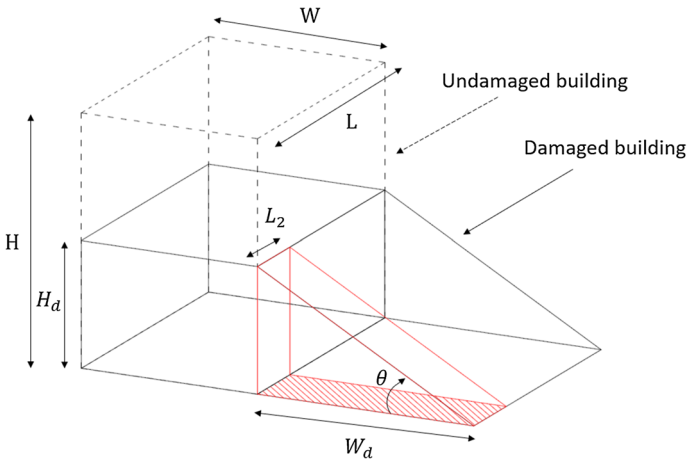

Fig. 2 Simplified debris model for a building at collapse adapted from Argyroudis et al. (2015)

located randomly around the building, such that the total debris volume was accounted for. Then, given the width of street, the percentage of debris coverage was calculated as the total surface area of debris divided by the area of street adjacent to the building.

As the final step, the model proposed in Lu et al. (2019) was utilized to calculate the reduction coefficients affecting the walking speed. Lu et al. (2019) conducted experimental tests to quantify the effect of falling debris on the pedestrian movement. The volunteers traveled the designated route with different levels of debris coverage, in which walking and running time were recorded to estimate the corresponding reduction coefficient. It was found that as the debris coverage exceeds 25%, individuals can hardly pass through the obstacles. Note that the reduction coefficient is based on the percentage of debris coverage associated with each building. The final reduction coefficient for each link or street was calculated based on the average reduction coefficient computed for buildings associated to that link. Finally, the total number of casualties and associated annualized risks are calculated under different policy alternatives resulting in selected decisions for the community. Note that although response and mitigation measures are often constrained by the availability of financial resources, this is not considered here as indicated by the dash decision box.

According to Modarres et al. (2016), the risk analysis consists of three main components: (1) selecting the hazardous event (2) determining likelihood or the probability of the occurrence of the event, (3) evaluating consequences or losses. As a result, in this study, the life safety risk is defined as the number of casualties multiplied by the probability of occurrence calculated as the inverse of the recurrence interval. The risk provides insight into events that result in both significant losses and have a high probability of occurrence. The proposed methodology is designed to be implemented within the Interdependent Networked Community Resilience Modeling Environment (IN-CORE), but for this paper the earthquake casualty, debris, and tsunami casualty algorithms were external to IN-CORE. IN-CORE is a robust, open-source computational platform developed by Center for Risk-Based Community Resilience Planning to integrate engineering and socioeconomic algorithms and model the impact of natural hazards to communities as well as their recovery, evaluate community resilience, and ultimately optimize

resilience strategies (Gardoni et al. 2018; van de Lindt et al. 2019). IN-CORE is freely available online and a Python library (pyIncore) is available for a variety of researchers from different disciplines.

4 Description of the example testbed

In this study, the city of Seaside, Oregon, is selected as an example community to illustrate the application of the methodology. Seaside is a city in Clatsop County, Oregon, located in the vicinity of CSZ and vulnerable to both seismic and tsunami hazards (Goldfinger et al. 2012; Oregon Seismic Safety Policy Advisory Commission 2013; Wood 2007). Previous studies have shown that Seaside has the highest vulnerability to tsunami hazards among Oregon coastal communities (Wood 2007; Wood et al. 2010). According to the 2020 US Census (2020), the total population of Seaside is estimated as 7115 people. However, similar to other coastal communities, since the tourism industry is the mainstay of the economy, the tourist population can be substantial in a single day, especially during the peak of summer hours (Connor 2005; Venturato 2005). Thus, in such circumstances, the tourist population fluctuation must be taken into account to achieve a realistic life safety risk assessment (Kellen et al. 2012; Mostafizi et al. 2017).

For Seaside, there have been a few historically recorded far-field tsunamis with the earthquake origin being in Alaska (1952 and 1964), Chile (1960), and Japan (2011). While there were no substantial human losses, the city has experienced economic losses. For example, the Alaska (1964) earthquake and tsunami caused $276 K damage to the city and private sectors (NHMP 2015). Recently, an official evacuation warning was issued in Seaside in 2011 due to the Japan (2011) earthquake that led to a mandatory city evacuation (Buylova et al. 2020). Following the 2011 Seaside evacuation warning, the Oregon Department of Geology and Mineral Industries (DOGAMI) has conducted extensive studies on the evacuation planning in Seaside leading to the tsunami evacuation map for the community (Priest et al. 2015). Seaside has a fairly flat topography, and the existing evacuation plan for areas inside the tsunami inundation zone requires the horizontal evacuation on foot to minimize the potential traffic congestion, and alternative options such as the vertical evacuation has only recently been discussed (Chen et al. 2020; Wang et al. 2016). This can be a major issue since most residents live on the west side of the Necanicum River, where they need to travel up to 1.5 km, passing one or more bridges to surpass the tsunami inundation zone.

Figure 3 shows the geographic location of Seaside with tsunami shelters (eight horizontal and one vertical shelters), transportation network (roads and bridges), buildings at the parcel level, and two street views of the area. It should be noted that while the existing tsunami evacuation plan for Seaside does not include the vertical evacuation, in this study, one vertical shelter located in the downtown area is considered among other mitigation strategies.

5 Simulation inputs

5.1 Decision support options

In this study, given the vulnerability of Seaside to the earthquake and near-field tsunami, the first step in decision and support option is to select the threatening probabilistic

Fig. 3 Relative Location of Seaside, OR: **a** transportation network and tsunami shelters; **b** downtown area enclosed by the red box (building type and corresponding code level); **c** street view 1 (downtown area); **d** street view 2 (Seaside beach)

hazards with associated severity in terms of the recurrence interval. Regarding the infrastructure system, the building and transportation network are selected as the vulnerable infrastructures that have considerable impacts on the life safety risk. Regarding the population layer, residents, employees, and the tourist population with different spatial distributions, namely, daytime and nighttime are considered. Finally, to reduce the casualty results and associated risks, several mitigation strategies can be evaluated. In this study, three mitigation strategies, namely seismic retrofitting, tsunami readiness, and vertical evacuation shelters are considered.

5.2 Hazard description

In this study, the results of the Probabilistic Seismic and Tsunami Hazard Analysis (PSTHA) performed in Park et al. (2017a) for the city of Seaside, Oregon are utilized. The PSTHA used a logic-tree-based approach to consider a full-rupture of the CSZ, and

consisted of three main models, including the earthquake source model, earthquake simulation model, and tsunami model. The earthquake fault source models and their characteristics were obtained using a tapered Gutenberg-Richer distribution (Rong et al. 2014). The seismic intensity measures were obtained through the earthquake simulation model using ground motion prediction equations (Abrahamson et al. 2016). Finally, given the earthquake source modeling, the tsunami hazards were obtained by solving the nonlinear shallow water equations (Lynett et al. 2002; Titov et al. 2011). The annual exceedance probabilities of both earthquake and tsunami hazards, such as peak ground acceleration (PGA), elastic spectral acceleration, maximum flow depth, and tsunami momentum flux were computed at the specific location. This analysis resulted in seismic and tsunami hazard maps associated with seven recurrence intervals, namely 100-, 250-, 500-, 1000-, 2500-, 5000-, and 10,000-years. Table 1 shows seven recurrence intervals and certain hazard information at the coast that are utilized as the simulation inputs for earthquake and tsunami casualty models.

5.3 Built environment

The built environment for Seaside consists of four infrastructure systems, including buildings, transportation network, electric power network, and water supply network (e.g., Kameshwar et al 2021; Sanderson et al. 2022a). In this study, buildings and transportation network (e.g., roads and bridges) were considered, and additional complications due to the other networks (e.g., loss of power, water leaks, potential for fire following earthquake) were not included. The building characteristics were primarily identified using tax lot data from Clatsop County. Secondary means of verification were done through a field survey of limited number of buildings and by spot-checking using Google Street View (Cox et al. 2022; Park et al. 2017b). A total of 4679 buildings were identified and classified as light frame wood buildings with the floor area less than 5000 sq. ft. (W1: 2446 parcels), any wood buildings with the floor area greater than 5000 sq. ft. (W2: 731 parcels), low-rise concrete moment frame buildings (C1L: 1039 parcels), and mid-rise concrete moment frame buildings (C1M: 465 parcels). Figure 4 shows the layout of building types at the parcel level in Seaside, Oregon.

Table 1 Recurrence intervals and corresponding hazard information

RI	AEP (%)	Seismic		Tsunami		
		PGA (g)	S_A(g)	T_0(min)	T_{Max}(min)	H_{max}(m)
100	1	0.10	0.17	39.0	40.0	3.0
250	0.4	0.43	0.87	38.5	41.5	4.4
500	0.2	0.60	1.25	38.0	45.0	7.3
1000	0.1	0.72	1.45	38.0	48.0	10.2
2500	0.04	0.9	1.8	37.2	46.0	12.2
5000	0.02	1.0	2.0	37.0	45.5	13.6
10,000	0.01	1.15	5.7	36.3	43.0	14.5

RI: recurrence interval; AEP: annual exceedance probability (1/RI); PGA: peak ground acceleration; S_A: spectral acceleration for W1 buildings (period = 0.35); T_0: arrival time (at the shoreline); T_{Max}: Max runup time (at the center line); H_{max}: maximum flow depth

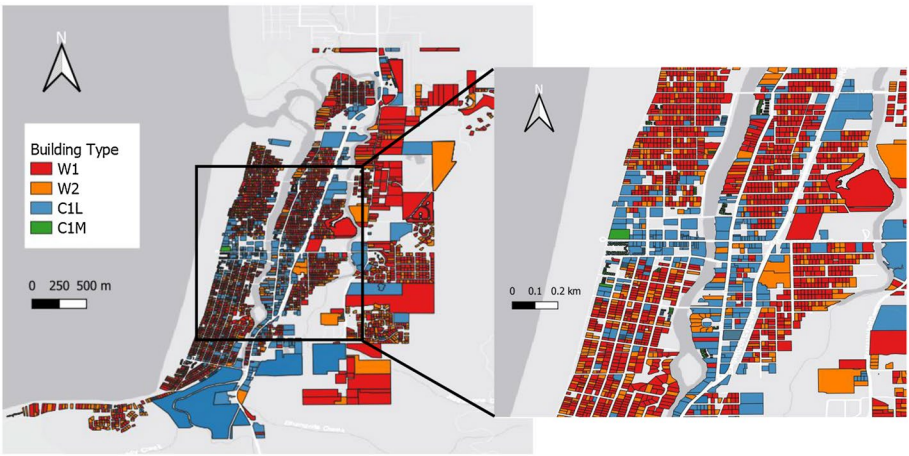

Fig. 4 Layout of building types at Seaside, Oregon (W1 is light framed wood buildings with the floor area less than 5000 sq. ft., W2 is any wood buildings with the floor area greater than 5000 sq. ft., C1L is low-rise concrete moment frame buildings, and C1M is mid-rise concrete moment frame buildings)

5.4 Social environment

In this study, nighttime and daytime population layers consisted of three population-related variables, including (1) residents, (2) employees, and (3) tourists. The resident population of Seaside was estimated as 6457 people according to the 2010 US Census. The method developed by Rosenheim et al. (2019) was adopted to assign demographic characteristics such as the number of people, tenure status, and race to individual household units, although not all characteristics were incorporated for this study. The process is based on the probabilistic housing unit allocation algorithm using US Census data at the block level to inform housing unit characteristics at the parcel level. The results consist of the number of people in housing units and information about the land use types, namely vacant, residential, commercial, and seasonal rental (Rosenheim 2021). The employee population for all businesses at the parcel level was estimated using Data Axle USA Database (2020).

The tourist population was estimated from combination of three sources: the Hatfield Marine Science Center (HMSC), Oregon State Parks (OSP), and overnight visitors (Dean Runyan Associates 2021). The HMSC, located in Newport, Oregon, operates a visitor center for public outreach on marine science and attracts a large number of tourists, particularly in summer months and on weekends between late Spring and early Fall. We assume that the seasonal (e.g., higher visitor counts in summer) and weekly (e.g., higher visitor counts on weekends) variation of daytime visitors is qualitatively similar to Seaside. The HMSC Visitor Center is closed on some occasions, and the average value of adjacent days was utilized to fill in the gaps. Weekly and daily ratios of visitors were calculated based on revised temporal data. The total number of daily visitors for Seaside was calculated based on the monthly OSP data for that area, which provided a means to scale the HMSC data. Finally, using the total monthly visitors from OSP combined with weekly and daily ratios from HMSC, the temporal fluctuation of visitors for daytime population was estimated.

Regarding nighttime population, Dean Runyan Associates (2021) provides a total estimate of overnight visitors for the Clatsop County in 2018, from which the monthly

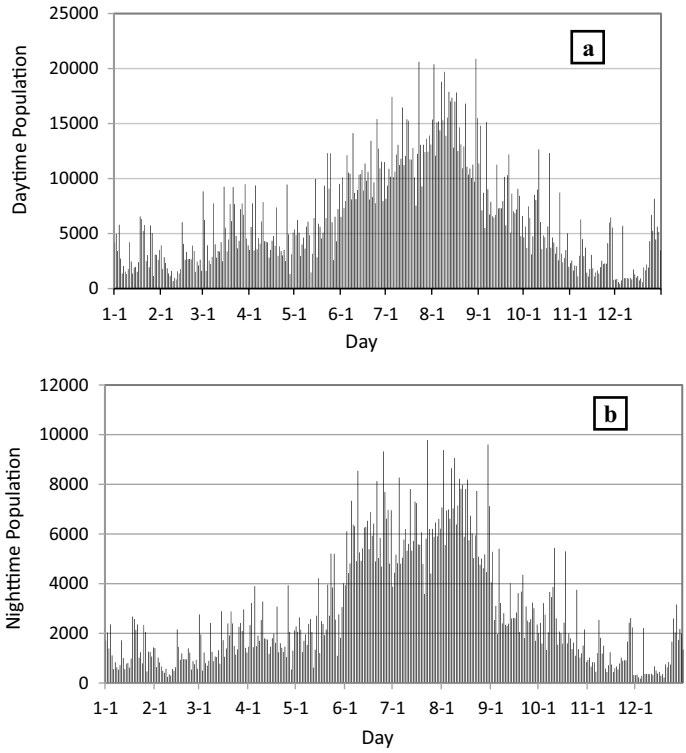

Fig. 5 The estimation of the temporal fluctuation of visitors for Seaside: **a** daytime population; **b** nighttime population

overnight visitors for Seaside was calculated based on its population compared to other cities in the county such as Astoria, Cannon Beach, Gearhart, and Warrenton. Finally, given similar weekly and daily ratios of visitors obtained from HMSC, the daily temporal fluctuation of overnight visitors for Seaside was estimated. Figure 5 shows the results in terms of the temporal fluctuation of visitors for daytime and nighttime population in Seaside. The maximum daytime and nighttime tourist population were estimated about 20,000 and 10,000, respectively, which appear to be reasonable based on previous studies (e.g., Connor 2005; Venturato 2005; Wang and Jia 2021; Wojahn 1976). Moreover, while the estimates could be refined in future studies, we emphasize that the intention of this work is to understand the overall life safety risk considering the addition of a realistic tourist population for a typical coastal city. We note that other cities for which tourism is a major industry may have different trends. Arrighi et al. (2022), for example, studied the flood risk for Florence, Italy, and assumed a constant annual influx of tourists.

Note that the maximum daytime and nighttime tourist populations of 20,000 and 10,000 were selected as the worst-case scenario to estimate the highest life safety risk. While the uncertainty in the initial population distribution is essential for the casualty model, it will be addressed in future studies where yearly population fluctuations will be considered. To develop the high-resolution population layer for the selected daytime and nighttime, certain allocation strategies were considered. For the daytime population, we assumed that 20% of residents would remain at home (Rosenheim et al. 2019;

Rosenheim 2021). Second, according to Data Axle USA Database (2020), there were 5103 employees who were allocated to target parcels. Finally, tourists were allocated in hotels with an occupancy rate of 45%, and the remaining tourist population was randomly distributed with 40% placed near the beach distributed normally around the centroid of the downtown area, 30% in the downtown area, and 30% in seasonal rentals. Note that we did not consider any person on the sand beach or in the water. For the case of Seaside, the water is generally too cold for swimming, and the number of tourists on the beach is typically much smaller than the number on the boardwalk or in the town. Future iterations of this model could consider the beach population since this group would have the greatest exposure to the tsunami hazard. Regarding the nighttime population, firstly, it assumed that 100% of residents would remain at home. Secondly, the tourists were randomly allocated in hotels (hotel occupancy = 90%), and seasonal rentals identified by the housing unit allocation method (Rosenheim 2021). Online data were used to determine the approximate number of rooms in 40 hotels and vacation homes in Seaside. Regarding the hotel capacity, it was assumed that there were on average 3 persons in each room. Figure 6 shows the heatmap for daytime and nighttime population at the parcel level including numbers of residents, employees, and tourists (peak summer weekend). As shown in Fig. 6a, the downtown area has a higher population during the daytime, which the maximum of density is 1.8 person/m^2. As shown in Fig. 6b, during the nighttime, the population layer is more uniform, and the maximum of density is 0.4 person/m^2 driven by multi-story hotels and seasonal rentals.

5.5 Probabilistic simulations

The probabilistic simulation consisted of four main modules (Fig. 1, Step 5), namely the building damage model, debris model, earthquake and tsunami casualty models. In this

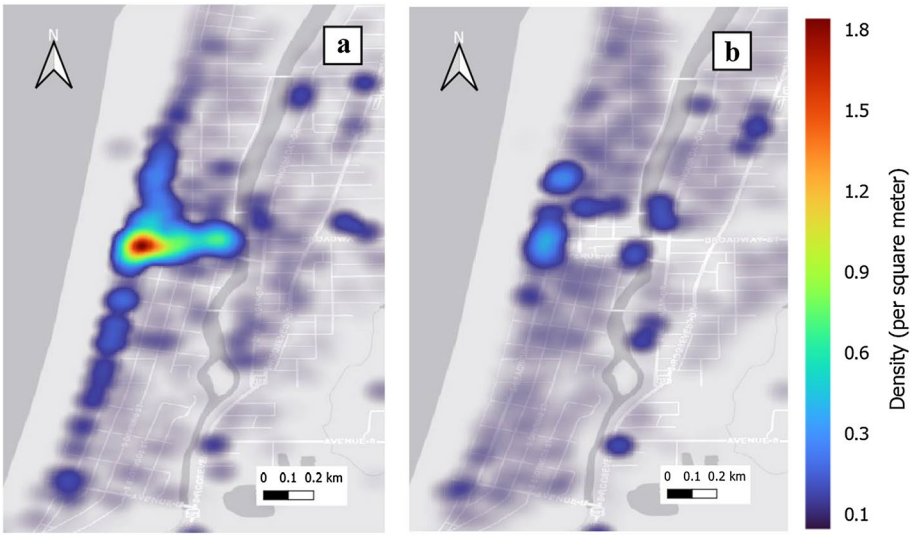

Fig. 6 The heatmap for the population distribution (residents, employees, and tourists) for city of Seaside, Oregon: **a** daytime population, **b** nighttime population

study, building damage due to earthquake and the subsequent debris were estimated and then utilized as the input for casualty models. Therefore, for the sake of brevity, these models are included in the scope of the casualty model and are not discussed individually. First, the earthquake casualty model was developed based on the HAZUS methodology. In this study, only buildings with associated indoor casualties were considered for the earthquake casualty model due to its higher vulnerability compared to bridges. Second, the tsunami casualty model was developed to explicitly incorporate two important variables, including the effect of earthquake-induced damage to buildings on building egress time, and the effect of earthquake-induced debris on the evacuation speed. The output of this study consists of the number of casualties (fatality and injury) for the selected population layer (daytime and nighttime) due to earthquake and tsunami hazards at the parcel level. The results were also compared to quantify the effect of different mitigation strategies on the resilience metrics for the community.

5.5.1 Earthquake casualty model

The HAZUS earthquake casualty model applies an event tree model to estimate the number of casualties due to only direct physical damage to buildings and bridges. It should be noted that the HAZUS classifies damage states into five categories: *none*, *slight*, *moderate*, *extensive*, and *complete*; however, IN-CORE is used for the damage analysis herein and is limited to four damage states: *none/insignificant* (DS0), *moderate* (DS1), *extensive* (DS2), and *complete* (DS3). Figure 7 shows an example of probabilities of exceeding DS0 and DS1 for the 500-year earthquake hazard corresponding to limit states LS0 and LS1, respectively. In this study, the casualties are estimated due to only direct physical damage to buildings in terms of the number of injury (*Severity 1* and *Severity2)* and fatality (*Severity 3* and *Severity 4)* at the parcel level and then aggregated in the study region. It should be noted that considering both *Severity 3* and *Severity 4* as the fatality is a conservative assumption, and it presumes that immediate treatment would not be available after the earthquake.

Fig. 7 Probability of exceeding specific damage state for the 500-year earthquake hazard: **a** LS0, **b** LS1

5.5.2 Tsunami casualty model

As mentioned earlier, the critical time in the tsunami casualty model consists of five variables, namely maximum runup time (T_{max}), time to issue warning (T_w), estimated preparation time (T_{prep}), travel time to safety (T_{travel}), and building egress time (T_{be}). For the city of Seaside, the variable T_{max} was estimated based on the PSTHA for different recurrence intervals (Table 1). The variable T_w was selected to be zero since currently there is no operational warning system for the near-field tsunami in Seaside. Regarding the variable of T_{prep}, given a good tsunami awareness program in Seaside (Connor et al. 2005), the level of preparedness was selected as fair (15 min) and good (10 min) for residential and tourist populations, respectively. There are other factors for the preparation time such as the choice of transportation mode and knowledge of the route that are not considered here (e.g., Mostafizi et al. 2019; Muhammad et al. 2021). The variable T_{travel} was estimate based on the shortest path to safety. Given the current evacuation plan for Seaside, the tsunami evacuation was only considered on foot, in which a normal distribution with a mean speed and standard deviation of 1.5 m/s and 0.2 m/s was selected, respectively (Wang et al. 2016). This would cover a range of speed from slow walking, fast walking, to slow running (TBR 2010). Note that given implementing a macroscopic model for the tsunami evacuation simulation, interactions among evacuees when traveling from the outside of buildings to shelters were neglected. Regarding the building egress time, the results of the agent-based model developed by Liu et al. (2016) were utilized to estimate the T_{be} for buildings impacted by the earthquake during the tsunami evacuation at the parcel level, in which the human evacuation behavior was considered in the estimated time. To estimate T_{be} as a random variable (see Eq. 3), the lognormal distribution was used as the probability distribution. Table 2 shows results of building evacuation time (minute per story) for two types of structure, including residential/seasonal rentals and hotels/commercial buildings. The variable T_{be} is determined for buildings based on the expected value utilizing the probability of being in each damage state (Fig. 7) multiplied by corresponding building evacuation time (Table 2).

As mentioned earlier, the effect of seismic debris was incorporated in the tsunami evacuation model as the reduction coefficients affecting the walking speed. Therefore, the weight of debris (in tons) from each building due to the earthquake was calculated. The model requires several inputs, including unit weight of structural/nonstructural elements, damage state probabilities for both structural and nonstructural elements, square footage of each building, and debris generated from different damage states (% of unit weight of element). Figure 8 shows debris weights for 500- and 5000-year earthquake at the parcel level. As shown in Fig. 8, the concrete moment frame buildings that are

Table 2 Building egress time (minute per story) for residential/seasonal rental and hotels/commercial buildings

Damage state	Residential and seasonal rental buildings		Hotels and commercial buildings	
	Mean	Standard deviation	Mean	Standard deviation
DS0 (slight)	1.56	0.09	2.44	0.15
DS1 (moderate)	1.59	0.25	2.48	0.21
DS2 (extensive)	3.28	1.6	4.61	1.47
DS3 (complete)	3.28	1.6	4.61	1.47

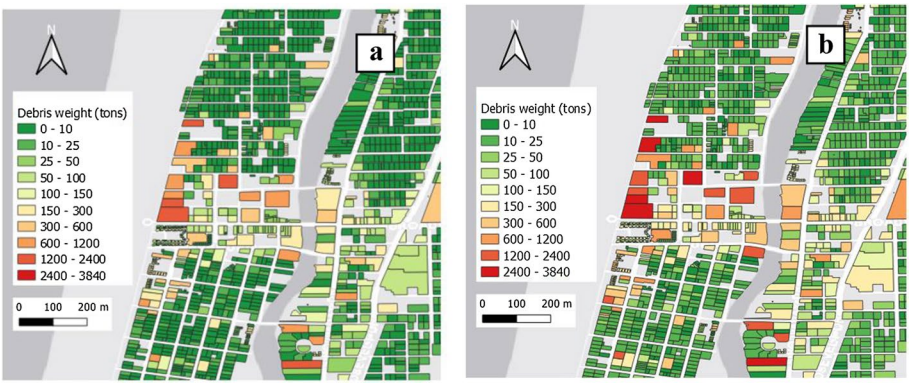

Fig. 8 Debris weight for selected recurrence intervals at the parcel level: **a** 500-year earthquake; **b** 5000-year earthquake

densely located in the downtown area are responsible for most of the debris weight (larger than 300 tons).

As the next step, given the debris weight, the total debris volume was calculated at the parcel level utilizing the density for heavy and light debris as 1.91 ton/m^3 and 0.45 ton/m^3, respectively. Similar to Fig. 8, the spatial distribution of the debris volume at the parcel level was calculated. Then, the debris volume was distributed randomly around the perimeter of the building. According to method proposed by Argyroudis

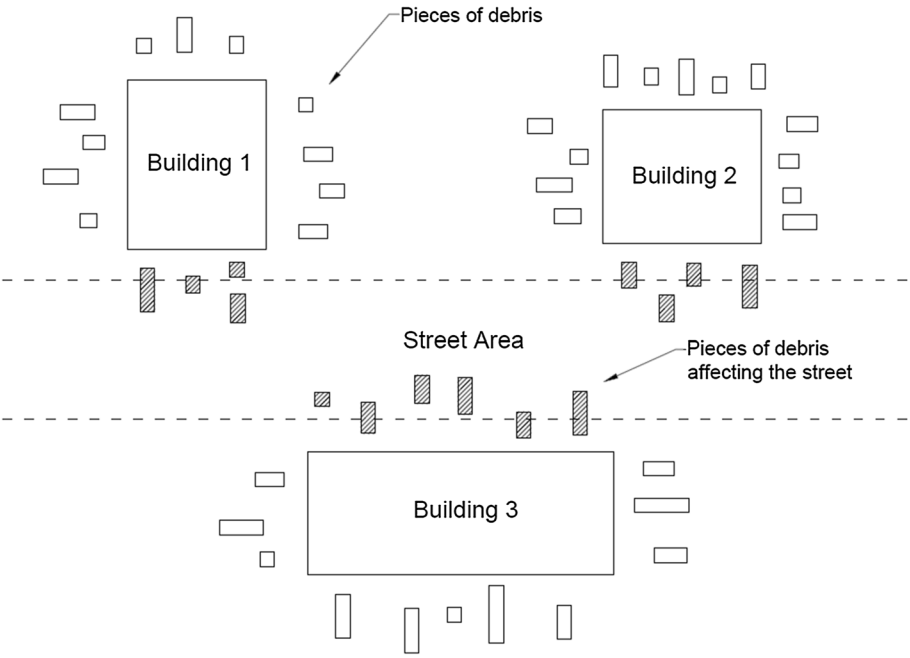

Fig. 9 Simplified illustration of the spatial distribution of debris pieces around buildings and the ones affecting the street area and the walking speed

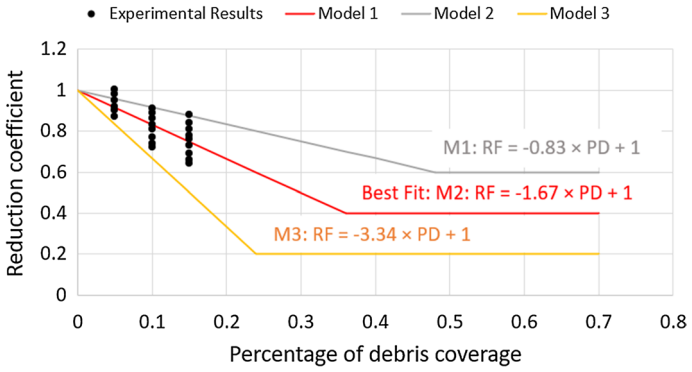

Fig. 10 Reduction coefficient versus percentage of debris coverage and fitted models (Lu et al. 2019)

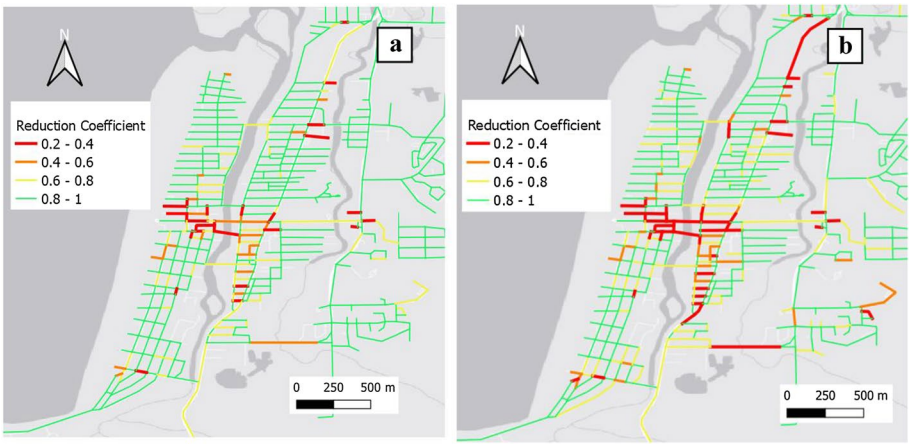

Fig. 11 The effect of earthquake-induced debris on the evacuation speed based on debris model M2: **a** reduction coefficients for 500-year earthquake; **b** reduction coefficients for 5000-year earthquake

et al. (2015), W_d was estimated using a normal distribution, and k_v and θ were assumed to be statistically independent (Eq. 4). The statistics of k_v and θ are: $\mu_{k_v} = 0.5$, $\sigma_{k_v} = 0.15$, $\mu_\theta = 45^\circ$, $\sigma_\theta = 13.5^\circ$. Finally, pieces of debris were located randomly around the building, with L2 (see Fig. 2) set equal to 0.5 m, such that the total debris volume was accounted for. Noted that while the sensitivity analysis showed that selecting L2 as a deterministic variable does not significantly affect the casualty results, such comparisons have not been presented for the sake of brevity. Figure 9 shows a simplified example of the spatial distribution of debris around buildings. Even though pieces of debris are randomly distributed around buildings, as shown in Fig. 9, the ones adjacent to the street are considered to affect the walking speed of evacuees. Finally, given the percentage of debris coverage with each building and the model proposed by Lu et al. (2019), the reduction coefficients for each link or street were calculated. Figure 10 shows the experimental results for the walking condition as black dots and models fitted in this in study. While the original model included a logarithmic-based regression, for our study, multiple debris models with different thresholds were investigated due to experimental

uncertainty and inherent uncertainty in human behavior. The sensitivity analysis was conducted to understand the effect of different debris models shown in Fig. 10 (M1, M2, and M3) on the casually results (Sect. 6.4 Sensitivity analysis). While the debris models M1 and M3 represent upper and lower bounds, the debris model M2 was selected as a representative case (the best fit) for most of the results and discussion in this paper.

Figure 11a, b shows the reduction coefficient for 500- and 5000-years earthquakes based on the debris model M2, respectively. The majority of links in the downtown area with a high concentration of concrete building constructed at low to moderated seismic code (Fig. 3b) have a reduction coefficient below 0.4 due to extensive earthquake damage (red links) resulting in a large amount of debris. As the intensity of the hazard increases, the reduction coefficient increases as expected. However, residential regions to the north and south of the central area have a majority wood-frame structures, which are less affected by seismicity and therefore generate less debris and less impact on the evacuation (green and yellow links). Figure 12 shows the number of people evacuating at each link during the daytime and nighttime. Clearly there are three streams of evacuees from the north, central and southern portions of the city. The central portion coincides with the downtown area where the reduction in walking speed is high due to debris (Fig. 11). The model estimates 3771 people in downtown area evacuate using one bridge where the corresponding reduction coefficients are 0.43 and 0.25 for 500- and 5000-years earthquakes, respectively.

6 Simulation results

6.1 Casualty modeling

Figure 13 shows the total number of casualties and associated risks due to the earthquake and tsunami for the baseline model with the nighttime population (no effect of earthquake damage on the tsunami evacuation). As shown in Fig. 13, the number of casualties (both fatalities and injuries) caused by the earthquake, as well as maximum associated risks, are significantly lower than those caused by the tsunami. This is because most buildings in Seaside are light-wood frame and are less vulnerable to earthquake compared to concrete

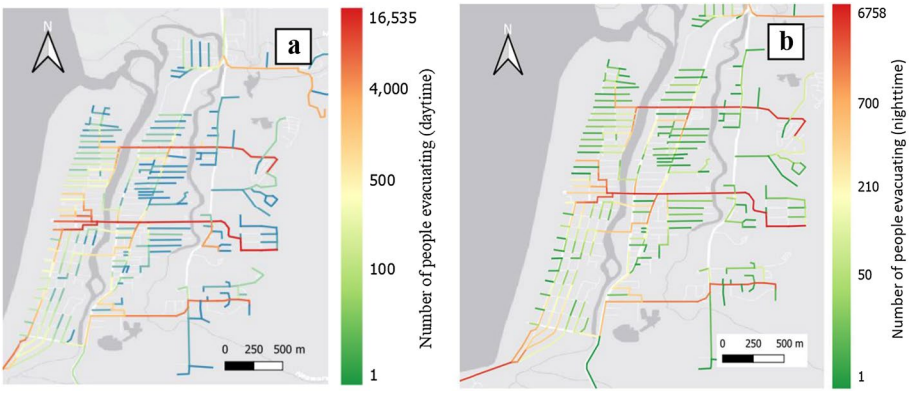

Fig. 12 The critical links and the number of people evacuation: **a** during the daytime; **b** during the nighttime

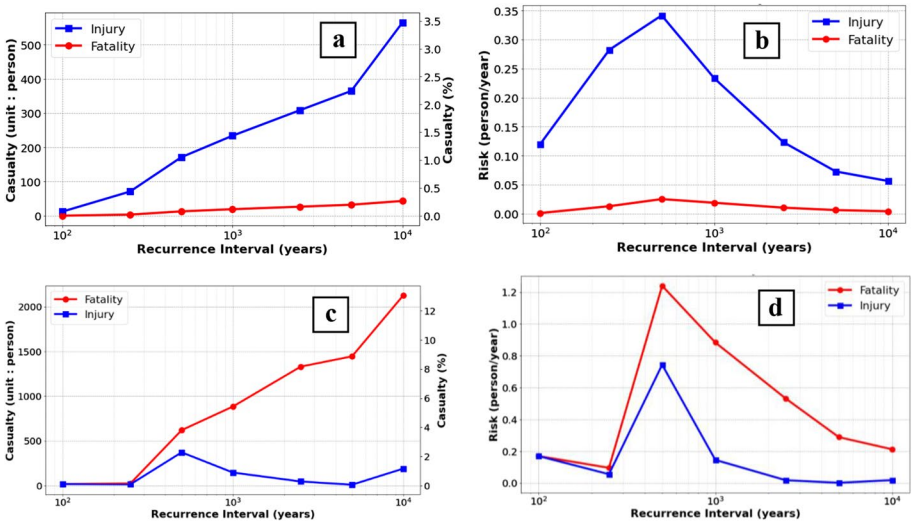

Fig. 13 Total number of casualties for the baseline model with nighttime population: **a** earthquake casualties, **b** earthquake risks, **c** tsunami casualties, **d** tsunami risks

buildings and because many of the concrete buildings were constructed with some level of seismic code. The number of injuries is higher than fatalities for all earthquake recurrence intervals as expected, and the maximum numbers of casualties occurring for the 10,000-year recurrence interval are 44 fatalities (0.3%) and 564 injuries (3.5%). Figure 13b shows that the highest casualty risk is associated with the 500-year recurrence interval. Note that since the total number of casualties due to the earthquake is insignificant, the population layer is assumed to be intact for the tsunami casualty model. While this assumption is justified for the city of Seaside, it can be adjusted for other case studies.

In contrast, Fig. 13c shows that for the tsunami, the number of fatalities is higher than injuries, particularly when the recurrence interval exceeds the 500-year recurrence interval. The maximum number of fatalities is 2127 persons (13.1%) occurring for the 10,000-year recurrence interval. This percentage is not unexpected for a nearfield tsunami. Suppasri et al. (2013) for example shows that fatality ratios were typically less than 15% for the Tohoku tsunami in Japan in 2011. Figure 13d shows that the maximum fatality and injury risks are 1.2 person/year and 0.75 person/year, respectively, which occurs also for the 500-year recurrence interval. At this recurrence interval, the tsunami life-safety risk is approximately 50 times larger for the tsunami compared to the earthquake, highlighting the importance of planning for evacuation for the tsunami. These results are based on the baseline model, in which the effect of earthquake-induced damage to buildings and associated debris are not considered. In addition, while similar results have been developed for the daytime population, the results are not presented here for the sake of brevity.

6.2 Impact of building evacuation and debris

Figure 14 compares the number of fatalities and associated annualized risk for the baseline case, the improved model considering the effect of the building damage on egress,

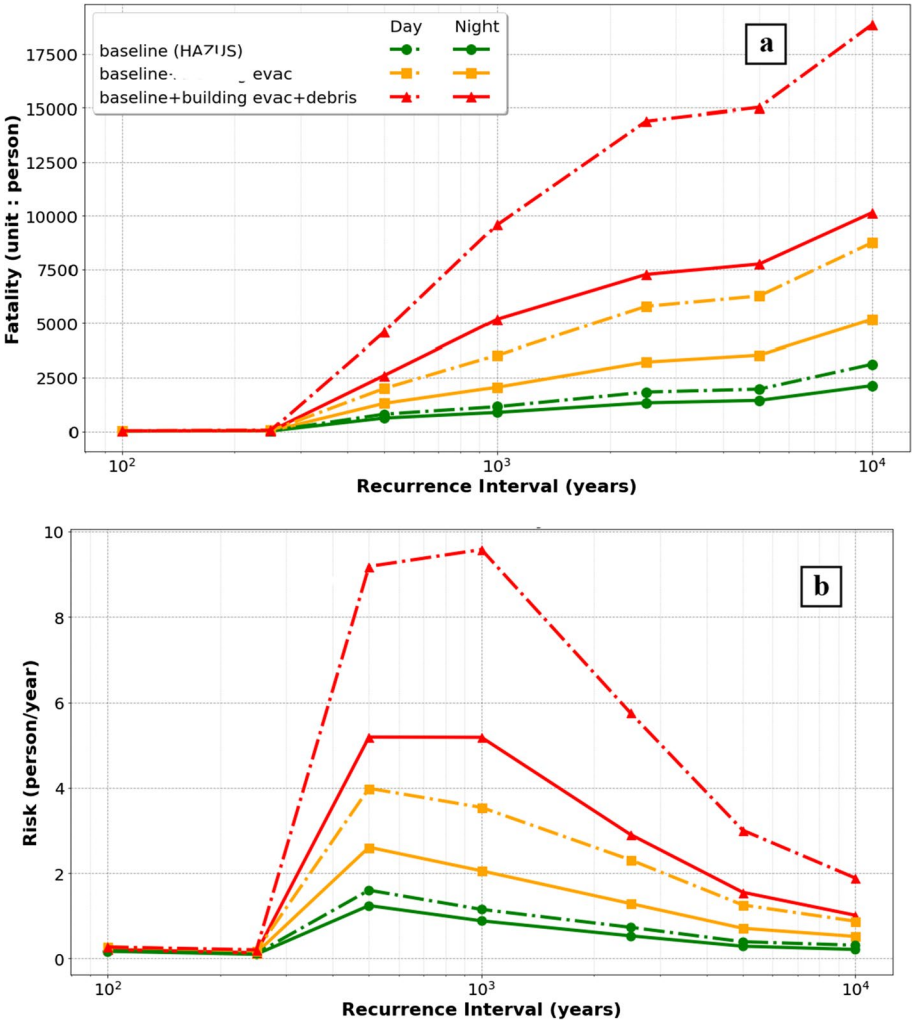

Fig. 14 The comparison between different models and population layer: **a** number of fatalities, **b** annualized fatality risk

and further improvement considering egress and horizontal evacuation. Similar to Fig. 13, the top panel shows the fatality count, and the lower panel shows the annualized risk. Figure 14 also compares two population layers for nighttime and daytime populations. As expected, the number of fatalities is negligible for the 100- and 250-year recurrence intervals since the tsunami inundation is almost negligible. The number of fatalities increases steadily as the recurrence interval increases, and the maximum risk is generally for the 500-year recurrence interval, although the 1000-year recurrence interval shows the 'worst risk case' when both egress and debris are included. The risk is higher for the daytime population since there are more people concentrated in the downtown area with concrete frame buildings that are more vulnerable to earthquake damage compared to wood frame buildings and because this area has a great exposure to the tsunami hazard. For example, for the 1000-year recurrence interval, the number

of fatalities during daytime population for baseline model is 1151 persons and increases to 3538 persons when the effect of earthquake-induced damage to the building is considered (33% increase). As the hazard intensity increases, the effect earthquake-induced damage to the building on the building evacuation and ultimately the number of fatalities become more significant.

The maximum number of fatalities occurs when the effect of earthquake-induced debris on the evacuation travel time is also considered, and the difference between daytime and nighttime population become more substantial (baseline + building evac + debris). For example, the number of fatalities for the 1000-year recurrence interval during the nighttime and daytime population is 5180 persons and 9577 persons, respectively. The substantial increase in the number of fatalities (85% for the 1000-year recurrence interval) is because the downtown area has the highest population density during the daytime and has highest reduction coefficients on the walking speed due to the large amount earthquake-induced debris. Similarly, as the hazard intensity increases, the effect earthquake-induced debris on the number of fatalities plays a larger role. Figure 14b shows the comparison of the annualized fatality risk for different models and population layers. The results indicate that although higher recurrence interval and magnitude results in a higher number of fatalities, the highest risks are associated with mid-range recurrence intervals. As the casualty model is improved in terms of considering effects of earthquake-induced damage to buildings and subsequent debris, the annual fatality risk increases, particularly for mid-range recurrence intervals. As a result, the highest fatality risks are 9.2 person/year and 9.6 person/year associated with the 500- and 1000-year recurrence intervals. Overall, Fig. 14b shows that when building egress and debris are considered for the worst risk cases (500- and 1000-year recurrence intervals), the annualized fatality risk increases by 4.2–8.3 times compared to the baseline case.

6.3 Mitigation strategies

Our model can be used to evaluate how different mitigation strategies, namely seismic retrofitting, tsunami readiness, and vertical evacuation shelters, can reduce the life safety risk. Mitigation measures are compared in terms of the number of fatalities and associated risks for the nighttime and daytime population. For the seismic retrofit of buildings, we assume that the design level of all building increases to the high code to decrease the level of seismic damage and subsequently amount of debris. For the tsunami readiness, we assume that there is a 5 min decrease in preparation time for both residents and tourists. Therefore,

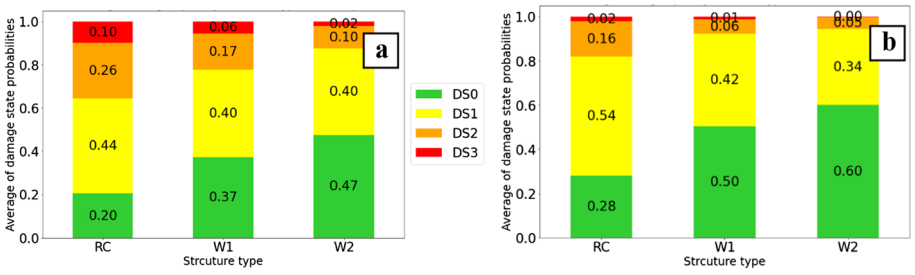

Fig. 15 Average of structural damage state probabilities observed for buildings grouped by the structure type: **a** status quo; **b** seismic retrofit

the residents and tourists start to evacuate in 10 min and 5 min, respectively. For the third alternative, we consider the construction of a vertical evacuation in the downtown area to reduce the travel time for the population based (e.g., Mostafizi et al. 2019). For this preliminary analysis, we do not consider relative costs for implementation, zoning regulations, or other social factors related to tsunami awareness or changes to risk perception.

Figure 15 shows the average of structural damage state probabilities for buildings grouped by the structure type between status quo and the seismic retrofit mitigation. As expected, the seismic retrofit mitigation decreases the number of structures of all types in the high damage states (DS2 and DS3). For example, regarding the RC buildings, the sum of averaged values of DS2 and DS3 for status quo and seismic retrofit are 0.36 and 0.18, resulting in a 50% reduction. Similarly, for the W1 and W2 buildings, the sum of averaged values of DS2 and DS3 is reduced by 70% and 58%, respectively.

Figure 16 shows the implication of seismic retrofit for the 500-year earthquake in terms of the debris generated at the parcel level and the subsequent reduction coefficients on the walking speed on specific links. When the design level of all buildings increases to high-code, the earthquake ground shaking damage to buildings and subsequent debris weight decrease significantly, particularly for reinforced concrete frame buildings with a high density in the downtown areas (Fig. 16a, b). Similarly, as shown

Fig. 16 The outputs of seismic retrofit for 500-year earthquake: **a** debris weight (status quo); **b** debris weight (seismic retrofit); **c** reduction coefficient (status quo); **d** reduction coefficient (seismic retrofit)

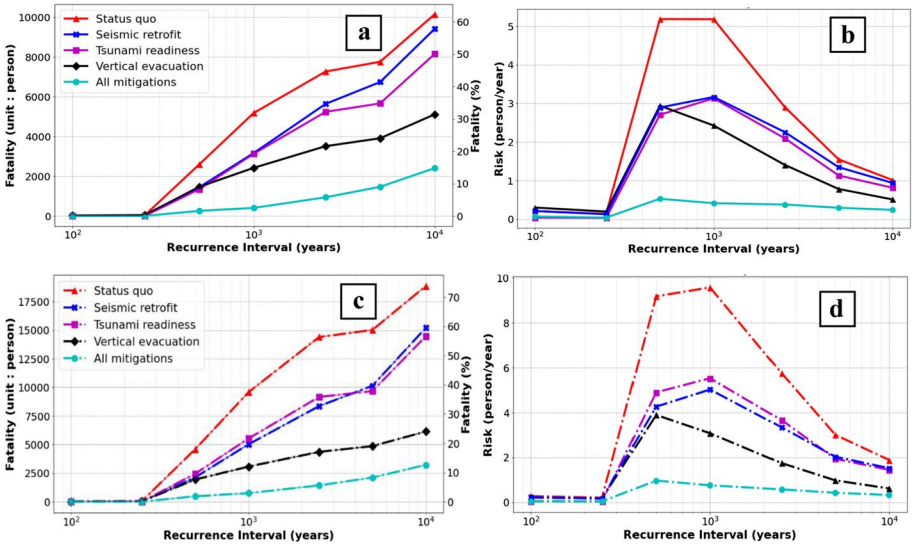

Fig. 17 The effect of different mitigation strategies: **a** number of fatalities for nighttime population **b** fatality risk for nighttime population; **c** number of fatalities for daytime population **d** the fatality risk for daytime population

in Fig. 16c, d, there is a significant impact on the reduction coefficient, particularly for links in the downtown area.

Figure 17 shows the effect of three mitigation strategies on the number of fatalities and associated risks for nighttime (a and b) and daytime (c and d) populations. Note that the scales are not the same between Fig. 17a, c and between Fig. 17b, d, and that the daytime population has significantly more risk for the reasons stated earlier. The results show that the seismic retrofit of buildings and the tsunami readiness have a similar reduction in the number of fatalities and risk for both nighttime and daytime populations. The vertical evacuation strategy is slightly more effective for recurrence intervals higher than 500-year. Considering all mitigation strategies together, the life safety risk for nighttime and daytime populations can be reduced substantially by 90% for the 500-year recurrence interval and by 92% reduction for 1000-year recurrence interval, respectively. As shown in Fig. 17c, d, a similar trend has been observed for the daytime population. The vertical evacuation strategy plays a more effective role in reducing the overall number of fatalities because the daytime population has a higher density in the downtown area where the vertical shelter is located. This exercise shows that multiple strategies may be necessary to reduce life safety risk in the event of a nearfield tsunami for urban coastal cities.

6.4 Sensitivity analysis

We conduct a sensitivity analysis to evaluate the effect of different levels of preparedness and earthquake debris models on the tsunami casualty results. As mentioned earlier, each level of preparedness corresponds to a specific preparation time for the community. Figure 18 shows the effect of the level of preparedness, namely Good (T_{prep}=10 min), Fair (T_{prep}=15 min), and Poor (T_{prep}=20 min) on the number of fatalities and casualties for the nighttime population. For the sensitivity analysis, the preparation time for the resident and tourist populations is considered the same. As shown in Fig. 18a, the number of fatalities

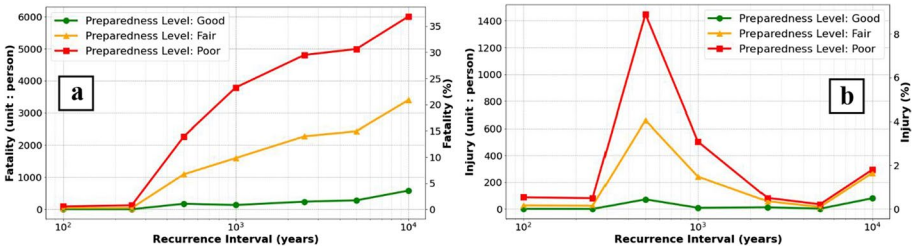

Fig. 18 The effect of preparedness level (Good: 10 min, Fair: 15 min, Poor: 20 min) on the casualty for the nighttime population: **a** number of fatalities; **b** number of injuries

is sensitive to the selected level of preparedness for all recurrence intervals higher than 250-year. For example, regarding the 1000-year tsunami, the number of fatalities for Good, Fair, and Poor levels of preparedness are 132 (0.8% of population), 1595 (9.8% of population), and 3788 (23.3% of population), respectively. This result is expected because the preparation level is essentially equated with the milling time, and there have been several studies to show how life safety correlates to milling time (e.g., Chen et al. 2022; Wang et al. 2016). For this case, milling time is the time between the ground shaking and the start of the evacuation. As mentioned earlier, there are other factors for preparedness such as the choice of transportation mode and knowledge of the route that are not considered here.

Figure 19 shows the effect of the debris model on the number of fatalities and casualties for the nighttime population. As it was expected, for 100- and 250-years seismic and tsunami recurrence intervals, the number of casualties is negligible due to the overall low amplitude of tsunami inundation. As shown in Fig. 19a, the number of fatalities is dependent on the selected debris model so that the its maximum belongs to the model M3, which reflects the highest reduction coefficient based on the percentage of debris coverage (Fig. 10). For example, for 1000-year recurrence intervals, the number of fatalities for models M1, M2, and M3 are 12%, 20%, and 30% of the nighttime population, respectively.

7 Discussion

This paper proposes a methodology to evaluate the effect of earthquake-induced damage to buildings and subsequent debris in the tsunami casualty modeling. The methodology includes several modules, namely decision support options, hazard description, social

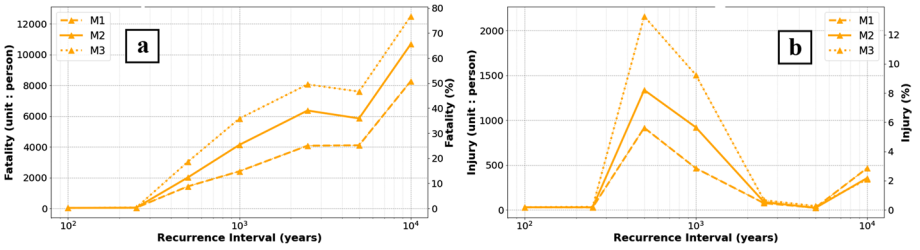

Fig. 19 The effect of debris model on the casualty for nighttime population with Fair level of preparedness: **a** number of fatalities; **b** number of injuries

environment, probabilistic simulations, annualized casualty risk, and finally selected decisions (Fig. 1). The city of Seaside, Oregon, vulnerable to the seismic earthquake and near-field tsunami due to CSZ, is selected as an example community to illustrate the application of the methodology. The results are compared in terms of the number of casualties and associated risk to quantify the effect of different mitigation strategies, namely seismic retrofitting, tsunami readiness, and vertical evacuation shelters.

The results indicate that the fatality and life safety risk of a near-field tsunami significantly increases when the effects of building egress and earthquake-induced debris are considered. The choice of population layer affects the life safety risk so that the maximum risk belongs to the daytime population. Furthermore, the number of fatalities is significantly reduced by using mitigation strategies. Interestingly, the seismic retrofit of buildings and the tsunami readiness have a similar mitigation effect on the number of fatalities, which indicates that investing in educating people to evacuate early is more cost-effective compared to the seismic retrofit of buildings. The findings not only aid in understanding the tsunami evacuation modeling, but also provide better insight for decision makers and emergency planners in coastal communities. Note that although socio-environmental and demographic variables for both nearfield and far-field tsunamis are beyond the scope of this paper, there are several studies for the reference (e.g., Buylova et al. 2020; Chen et al. 2021, 2022; Demuth et al. 2016; Lindell and Perry 2011).

This study has several limitations in the methodology and its application. First, given implementing a macroscopic model for the tsunami evacuation simulation, interactions among evacuees are neglected, which can negatively affect the outcomes (e.g., Wang et al. 2016; Mostafizi et al. 2019; Muhammad et al. 2021). For example, unlike the ABM, the evacuation curve including time along the horizontal axis cannot be developed in the macroscopic model due to its limitations. Second, the tsunami evacuation is only considered on foot and other modes of transportation are not considered in this study. This assumption can be justified for the case study since the current evacuation plan for Seaside requires only the horizontal evacuation on foot to minimize the potential traffic congestion during the evacuation (Wang et al. 2016; Chen et al. 2020). Third, although the earthquake-induced damage on bridges is not considered here, this topic has been covered in the past (e.g., Capozzo et al. 2019; Mostafizi et al. 2017; Priest et al. 2016). Finally, although different types of uncertainty are considered here in the casualty model, more studies are needed to identify the effect of potential uncertainties in the initial population distribution and the distribution of debris on the casualty results.

As potential highlights for future research, first, yearly population fluctuation should be considered to assess the casualty and associated risks. Second, a cost–benefit analysis needs to be implemented for different mitigation strategies in order to provide better insight for decision makers. Third, a targeted seismic retrofit of selected vulnerable buildings needs to be included to minimize the cost and maximize the effect of mitigation strategy. For example, the same level of life safe may be achieved by retrofitting only vulnerable buildings that are mostly concrete buildings located in the downtown area. Fourth, the casualty model can be coupled with models of urban change to evaluate life safety risks resulting from policy choices in coastal communities (Sanderson et al. 2022b). Last, future studies need to include behavioral interactions among evacuees such as congestion effects, panic, and herding behavior to represent a more realistic evacuation model (e.g., Wang et al. 2016; Mostafizi et al. 2017, 2019; Na and Banerjee 2019).

8 Conclusions

This study proposed a methodology to evaluate the life safety risk of coastal community vulnerable to earthquake and tsunami hazards. The work explicitly incorporated two important aspects in the tsunami evacuation modeling, including the effect of earthquake-induced damage to buildings on building egress time and associated earthquake-induced debris on horizontal evacuation time. The city of Seaside, Oregon, vulnerable to near-field earthquakes and tsunamis due to CSZ, was selected for the case study. Given the importance of the tourist industry in Seaside, the population layer accounted for not only residents, but also employees and tourists at the parcel level. The casualty rates were calculated for each parcel considering different community preparedness levels as well as daytime and nighttime population layers. The number of casualties and associated risks were compared to investigate the effect of different mitigation strategies, namely improving tsunami readiness, using vertical evacuation shelters, and seismic retrofitting methods on the life safety. Finally, a sensitivity analysis was performed to evaluate the effect of different levels of tsunami preparedness and earthquake debris models on tsunami casualty results. The main conclusions from this work are:

1. The results show that given the built environment characteristics in Seaside, in which the majority of buildings are wood-frame structures, the number of casualties and associated risk caused by the tsunami are significantly higher than those caused by the earthquake. The life safety risk of the tsunami significantly increases by 4.2–8.3 times when the effect of seismic damage to buildings on building egress time and earthquake-induced debris on horizontal evacuation time are considered (Fig. 14b). Note that even though the choice of population layer affects, namely nighttime and daytime populations can affect the life safety risk, its peaks occur at mid-range recurrence intervals, namely 500- and 1000-year recurrence intervals, respectively.
2. The number of fatalities is significantly reduced by using mitigation strategies; for example, as the tsunami readiness is improved, the highest fatality risk for the nighttime population is reduced by 48% associated with the 500-year recurrence interval. While the seismic retrofit of buildings and the tsunami readiness have similar mitigation effects, for extreme hazard intensities, with a recurrence interval larger than 500-year, the vertical evacuation strategy is most effective in reducing fatalities. Remarkably, considering all mitigation strategies together, the highest fatality risks for nighttime and daytime populations are reduced considerably by 90% and 92% associated with the 500- and 1000-year recurrence intervals, respectively.
3. The sensitivity analysis indicates that the choice of tsunami preparedness levels and corresponding preparation time (Good: 10 min, Fair: 15 min, Poor: 20 min) and debris models (M1, M2, and M3) in the casualty modeling can significantly affect the fatality results. For example, regarding the 1000-year tsunami, the number of fatalities for Good, Fair, and Poor levels of preparedness are 132 (0.8% of population), 1595 (9.8% of population), and 3788 (23.3% of population), respectively.

The methodology presented in this paper highlights the severe effect of seismic damage to building and resulting debris on the tsunami evacuation. Note that while this paper considered the impact of the CSZ on the city of Seaside, the methodology presented is generalizable to other communities with specific social characteristics.

Funding This work was funded by the cooperative agreement 70NANB15H044 between the National Institute of Standards and Technology (NIST) and Colorado State University through a subaward to Oregon State University and the Civil and Construction Engineering Graduate Fellowship from Oregon State University. The content expressed in this paper are the views of the authors and do not necessarily represent the opinions or views of NIST.

Data availability The datasets for Seaside, Oregon, including built-, natural-, and social-systems are available in the DesignSafe: https://www.designsafe-ci.org/data/browser/public/designsafe.storage.published/PRJ-3390. Other data and codes, including the earthquake and tsunami casualty models are available from the author upon reasonable request.

Declarations

Conflict of interest The authors have no conflicts of interest to declare with respect to the content of this article.

References

Abrahamson N, Gregor N, Addo K (2016) BC Hydro ground motion prediction equations for subduction earthquakes. Earthq Spectra 32:23–44. https://doi.org/10.1193/051712EQS188MR

Aguirre P, Vásquez J, de la Llera JC, Gonzalez J, Gonzalez G (2018) Earthquake damage assessment for deterministic scenarios in Iquique, Chile. Nat Hazards 92:1433–2146. https://doi.org/10.1007/s11069-018-3258-3

Alam MS, Barbosa AR, Scott MH, Cox DT, van de Lindt JW (2018) Development of physics-based tsunami fragility functions considering structural member failures. ASCE J Struct Eng. https://doi.org/10.1061/(ASCE)ST.1943-541X.0001953

Arrighi C, Carraresi A, Castelli F (2022) Resilience of art cities to flood risk: a quantitative model based on depth-idleness correlation. J Flood Risk Manag 15(2):e12794. https://doi.org/10.1111/jfr3.12794

Argyroudis S, Selva J, Gehl P, Pitilakis K (2015) Systemic seismic risk assessment of road networks considering interactions with the built environment. Comput Aid Civ Infrastruct Eng 30:524–540. https://doi.org/10.1111/mice.12136

Attary N, van de Lindt J, Unnikrishnan V, Barbosa AR, Cox D (2016) Methodology for development of physics-based tsunami fragilities. ASCE J Struct Eng. https://doi.org/10.1061/(ASCE)ST.1943-541X.0001715

Attary N, Unnikrishnan V, van de Lindt J, Cox D, Barbosa AR (2017) Performance-based tsunami engineering methodology for risk assessment of structures. Eng Struct 141:676–686. https://doi.org/10.1016/j.engstruct.2017.03.071

Attary N, van de Lindt JW, Barbosa AR, Cox DT, Unnikrishnan VU (2021) Performance-based tsunami engineering for risk assessment of structures subjected to multi-hazards: tsunami following earthquake. J Earthq Eng. https://doi.org/10.1080/13632469.2019.1616335

Badal J, Vázquez-Prada M, González Á (2005) Preliminary quantitative assessment of earthquake casualties and damages. Nat Hazards 34:353–374. https://doi.org/10.1007/s11069-004-3656-6

Bernardini G, Lovreglio R, Quagliarini E (2019) Proposing behavior-oriented strategies for earthquake emergency evacuation: a behavioral data analysis from New Zealand, Italy and Japan. Saf Sci 116:295–309. https://doi.org/10.1016/j.ssci.2019.03.023

Bernardini G, Ferreira TM (2022) Combining structural and non-structural risk-reduction measures to improve evacuation safety in historical built environments. Int J Archit Herit 16(6):820–838. https://doi.org/10.1080/15583058.2021.2001117

Buylova A, Chen C, Cramer LA, Wang H, Cox DT (2020) Household risk perceptions and evacuation intentions in earthquake and tsunami in a Cascadia subduction zone. Int J Disaster Risk Reduct 44:101442. https://doi.org/10.1016/j.ijdrr.2019.101442

Capozzo M, Rizzi A, Cimellaro GP, Domaneschi M, Barbosa A, Cox D (2019) Multi-hazard resilience assessment of a coastal community due to offshore earthquakes. J Earthq Tsunami 13(02):1950008. https://doi.org/10.1142/S1793431119500088

Carlos-Arce RS, Onuki M, Esteban M, Shibayama T (2017) Risk awareness and intended tsunami evacuation behavior of international tourists in Kamakura City, Japan. Int J Disaster Risk Reduct 23:178–192. https://doi.org/10.1016/j.ijdrr.2017.04.005

Castro S, Poulos A, Herrera JC, de la Llera JC (2019) Modeling the impact of earthquake-induced debris on tsunami evacuation times of coastal cities. Earthq Spectra 35(1):137–158. https://doi.org/10.1193/101917EQS218M

Chaoxu X, Gaozhong N, Xiwei F, Huayue L, Junxue Z, Xun Z (2022) A new model for the quantitative assessment of earthquake casualties based on the correction of anti-lethal level. Nat Hazards 110:1199–1226. https://doi.org/10.1007/s11069-021-04988-z

Charnkol T, Tanaboriboon Y (2006) Tsunami evacuation behavior analysis: one step of transportation disaster response. IATSS Res 30(2):83–96. https://doi.org/10.1016/S0386-1112(14)60173-4

Chen C, Buylova A, Chand C, Wang H, Cramer LA, Cox DT (2020) Households' intended evacuation transportation behavior in response to earthquake and tsunami hazard in a Cascadia Subduction Zone city. Transp Res Rec J Transp Res Board. https://doi.org/10.1177/0361198120920873

Chen C, Lindell MK, Wang H (2021) Tsunami preparedness and resilience in the Cascadia Subduction Zone: a multistage model of expected evacuation decisions and mode choice. J Disaster Risk Reduct 59:102244. https://doi.org/10.1016/j.ijdrr.2021.102244

Chen C, Mostafizi A, Wang H, Cox D, Cramer L (2022) Evacuation behaviors in tsunami drills. Nat Hazards 112:845–871. https://doi.org/10.1007/s11069-022-05208-y

Connor D (2005) The city of Seaside's Tsunami awareness program. Oregon Department of Geology and Mineral Industries. http://www.oregongeology.org/pubs/ofr/O-05-10_onscreen.pdf. Accessed 24 June 2014

Christoskov L, Samardjieva E (1984) An approach for estimation of the possible number of casualties during strong earthquakes. Bulg Geophys J 4:94–106

Cox D, Barbosa A, Alam M, Amini M, Kameshwar S, Park H, Sanderson D (2022) Seaside testbed data inventory for infrastructure, population, and earthquake-tsunami hazard. DesignSafe-CI. https://doi.org/10.17603/ds2-sp99-xv89

Cremen G, Galasso C, McCloskey J (2022) Modelling and quantifying tomorrow's risks from natural hazards. Sci Total Environ 817:152552. https://doi.org/10.1016/j.scitotenv.2021.152552

Data Axel (2020) Technical overview: data axel reference solutions—historical database. https://referencesolutions.data-axle.com/wp-content/uploads/2020/09/us-historical-business-1.pdf

Dean Runyan Associates (2021) The economic impact of travel in Oregon [PowerPoint Slides]. Travel Oregon. Accessed 20 June 2022. https://industry.traveloregon.com/wp-content/uploads/2021/05/OR_2020_Final.pdf

Demuth JL, Morss RE, Lazo JK, Trumbo C (2016) The effects of past hurricane experiences on evacuation intentions through risk perception and efficacy beliefs: a mediation analysis. Weather Clim Soc 8:327–344. https://doi.org/10.1175/WCAS-D-15-0074.1

Federal Emergency Management Agency (2013) Tsunami methodology technical manual. Washington, DC

Federal Emergency Management Agency (2015) HAZUS–MH 2.1 Technical manual. Washington, DC

Fraser S, Wood N, Johnston D, Leonard G, Greening P, Rossetto T (2014) Variable population exposure and distributed travel speeds in least-cost Tsunami evacuation modelling. Nat Hazards Earth Syst Sci 14:2975–2991. https://doi.org/10.5194/nhess-14-2975-2014

Freire S, Aubrecht C, Wegscheider S (2013) Advancing tsunami risk assessment by improving spatio-temporal population exposure and evacuation modeling. Nat Hazards 68(3):1311–1324. https://doi.org/10.1007/s11069-013-0603-4

Fritz HM, Petroff CM, Catalan PA, Cienfuegos R, Winckler P, Kalligeris N, Weiss R, Barrientos SE, Meneses G, Valderas-Bermejo C, Ebeling C, Papadopoulos A, Contreras M, Almar R, Dominguez JC, Synolakis CE (2011) Field Survey of the 27 February 2010 Chile Tsunami. Pure Appl Geophys 168:1989–2010. https://doi.org/10.1007/s00024-011-0283-5

Frucht E, Salamon A, Rozelle J, Levi T, Calvo R, Avirav V, Burns JN, Zuzak C, Gal E, Trapper P, Galanti B, Bausch D (2021) Tsunami loss assessment based on Hazus approach—the Bat Galim, Israel, case study. Eng Geol 289:106175. https://doi.org/10.1016/j.enggeo.2021.106175

Furukawa A, Spence R, Ohta Y, So E (2010) Analytical study on vulnerability functions for casualty estimation in the collapse of adobe buildings induced by earthquake. Bull Earthq Eng 8(2):451–479. https://doi.org/10.1007/s10518-009-9156-z

Gardoni P, van de Lindt J, Ellingwood B, McAllister T, Lee J, Cutler H, Cox D (2018) The interdependent networked community resilience modeling environment (IN-CORE). In: 16th European conference on earthquake engineering, Thessaloniki, GR

Goldfinger C, Nelson C, Morey A, Johnson J, Patton J, Karabanov E, Gutiérrez-Pastor J, Eriksson A, Gràcia E, Dunhill G, Enkin R, Dallimore A, Vallier T (2012) Turbidite event history—methods and implications for Holocene Paleoseismicity of the Cascadia Subduction Zone. U S Geol Surv Sci Prof Pap. https://doi.org/10.3133/pp1661F

Gu Z, Liu Z, Shiwakoti N, Yang M (2016) Video-based analysis of school students' emergency evacuation behavior in earthquakes. Int J Disaster Risk Reduct 18:1–1. https://doi.org/10.1016/j.ijdrr.2016.05.008

Hamacher HW, Tjandra SA (2002) Mathematical modelling of evacuation problems—a state of the art. Pedestrian Evacuat Dyn 24:227–266

Heaton TH, Hartzell SH (1987) Earthquake hazards on the Cascadia subduction zone. Science 236(4798):162–168. https://doi.org/10.1126/science.236.4798.162

Henry KD, Wood NJ, Frazier TG (2017) Influence of road network and population demand assumptions in evacuation modeling for distant tsunamis. Nat Hazards 85:1665–1687. https://doi.org/10.1007/s11069-016-2655-8

Kameshwar S, Cox DT, Barbosa AR, Farokhnia K, Park H, Alam MS, van de Lindt JW (2019) Probabilistic decision-support framework for community resilience: Incorporating multi-hazards, infrastructure interdependencies, and resilience goals in a Bayesian network. Reliab Eng Syst Saf 191:106568. https://doi.org/10.1016/j.ress.2019.106568

Kameshwar S, Park H, Cox D, Barbosa AR (2021) Effect of disaster debris, floodwater pooling duration, and bridge damage on immediate post-tsunami connectivity. Int J Disaster Risk Reduct 56:102119. https://doi.org/10.1016/j.ijdrr.2021.102119

Katada T, Kuwasawa N, Yeh H, Pancake C (2006) Integrated simulation of tsunami hazards. In: 100th anniversary earthquake conference including the 8th U.S. National Conference on Earthquake Engineering (8NCEE), the SSA Centennial Meeting, and the OES Disaster Resistant California Conference, No. 1727. San Francisco, California

Kellens W, Neutens T, Deckers P, Reyns J, Maeyer PD (2012) Coastal flood risks and seasonal tourism: analyzing the effects of tourism dynamics on casualty calculations. Nat Hazards 60:1211–1229. https://doi.org/10.1007/s11069-011-9905-6

Lammel G (2011) Escaping the tsunami: evacuation strategies for large urban areas concepts and implementation of a multi-agent based approach. Ph.D. thesis, Technische Universität Berlin

Levi T, Bausch D, Katz O, Rozelle J, Salamon A (2015) Insights from Hazus loss estimations in Israel for Dead Sea transform earthquakes. Nat Hazards 75:365–388. https://doi.org/10.1007/s11069-014-1325-y

Lindell MK, Perry RW (2011) The protective action decision model: theoretical modifications and additional evidence. Risk Anal 32(4):616–632. https://doi.org/10.1111/j.1539-6924.2011.01647.x

Liu J, Lin J (2012) Study on assessment method for earthquake casualty based on epicentral intensity. J Nat Disasters 21(5):113–119

Liu Z, Jacques C, Szyniszewski S, Guest J, Schafer B, Igusa T, Mitrani-Reiser J (2016) Agent-based simulation of building evacuation after an earthquake: coupling human behavior with structural response. Nat Hazards Rev 17(1):04015019. https://doi.org/10.1061/(ASCE)NH.1527-6996.0000199

Lu XZ, Yang ZB, Cimellaro GP, Xu Z (2019) Pedestrian evacuation simulation under the scenario of earthquake-induced falling debris. Saf Sci 114:61–71. https://doi.org/10.1016/j.ssci.2018.12.028

Lynett P, Wu T, Liu P (2002) Modeling wave runup with depth-integrated equations. Coast Eng 46:89–107. https://doi.org/10.1016/S0378-3839(02)00043-1

Natural Hazards Mitigation Plan (NHMP) (2015) Oregon natural hazards mitigation plan. https://www.oregon.gov/lcd/NH/Documents/Approved_2015ORNHMP.pdf

Nastev M, Todorov N (2013) Hazus: a standardized methodology for flood risk assessment in Canada. Can Water Resour J 38(3):223–231. https://doi.org/10.1080/07011784.2013.801599

Ma Y, Xie L (2000) Methodologies for assessment of earthquake casualty. Earthq Eng Vib 20(4):140–147

Macal CM, North MJ (2010) Tutorial on agent-based modelling and simulation. J Simul 4:151–162. https://doi.org/10.1057/jos.2010.3

Makinoshima F, Imamura F, Oishi Y (2020) Tsunami evacuation processes based on human behavior in past earthquakes and tsunamis: a literature review. Prog Disaster Sci 7:100113. https://doi.org/10.1016/j.pdisas.2020.100113

Mas E, Suppasri A, Imamura F, Koshimura S (2012) Agent-based simulation of the 2011 Great East Japan earthquake/tsunami evacuation: an integrated model of tsunami inundation and evacuation. J Nat Disaster Sci 34(1):41–57. https://doi.org/10.2328/jnds.34.41

Mas E, Koshimura S, Imamura F, Suppasri A, Muhari A, Adriano B (2015) Recent advances in agent-based tsunami evacuation simulations: case studies in Indonesia, Thailand, Japan and Peru. Pure Appl Geophys 172(12):3409–3424. https://doi.org/10.1007/s00024-015-1105-y

Mimura N, Yasuhara K, Kawagoe S (2011) Damage from the Great East Japan Earthquake and Tsunami—a quick report. Mitig Adapt Strateg Glob Change 16:803–818. https://doi.org/10.1007/s11027-011-9297-7

Mls K, Kořínek M, Štekerová K, Tučník P, Bureš V, Čech P, Husáková M, Mikulecký P, Nacházel T, Ponce D, Zanker M (2022) Agent-based models of human response to natural hazards: systematic review of tsunami evacuation. Nat Hazards. https://doi.org/10.1007/s11069-022-05643-x

Modarres M, Kaminskiy M, Krivtsov V (2016) Reliability engineering and risk analysis: a practical guide. CRC Press, Boca Raton

Mostafizi A, Wang H, Cox D, Cramer LA, Dong S (2017) Agent-based tsunami evacuation modeling of unplanned network disruptions for evidence-driven resource allocation and retrofitting strategies. Nat Hazards 88(3):1347–1372. https://doi.org/10.1007/s11069-017-2927-y

Mostafizi A, Wang H, Cox D, Dong S (2019) An agent-based vertical evacuation model for a near-field tsunami: choice behavior, logical shelter locations, and life safety. Int J Disaster Risk Reduct 34:467–479. https://doi.org/10.1016/j.ijdrr.2018.12.018

Muhammad A, Goda K, Alexander NA, Kongko W, Muhari A (2017) Tsunami evacuation plans for future megathrust earthquakes in Padang, Indonesia, considering stochastic earthquake scenarios. Nat Hazards Earth Syst Sci 17:2245. https://doi.org/10.5194/nhess-17-2245-2017

Muhammad A, De Risi R, De Luca F, Mori N, Yasuda T, Goda K (2021) Are current tsunami evacuation approaches safe enough? Stoch Environ Res Risk Assess 35:759–779. https://doi.org/10.1007/s00477-021-02000-5

Na HS, Banerjee A (2019) Agent-based discrete-event simulation model for no-notice natural disaster evacuation planning. Comput Ind Eng 129:44–55. https://doi.org/10.1016/j.cie.2019.01.022

Neumann B, Vafeidis AT, Zimmermann J, Nicholls RJ (2015) Future coastal population growth and exposure to sea-level rise and coastal flooding–a global assessment. PLoS ONE 10(3):e0118571. https://doi.org/10.1371/journal.pone.0118571

Okal EA (2015) The quest for wisdom: lessons from 17 tsunamis, 2004–2014. Phil Trans R Soc A 373:20140370. https://doi.org/10.1098/rsta.2014.0370

Oregon Seismic Safety Policy Advisory Commission (2013) The Oregon Resilience Plan: reducing risk and improving recovery for the next Cascadia earthquake and tsunami. Portland, Oregon

Park H, Cox D, Alam M, Barbosa A (2017a) Probabilistic seismic and tsunami hazard analysis conditioned on a megathrust rupture of the Cascadia subduction zone. Front Built Environ 3:1–19. https://doi.org/10.3389/fbuil.2017.00032

Park H, Cox D, Barbosa A (2017b) Comparison of inundation depth and momentum flux-based fragilities for probabilistic tsunami damage assessment and uncertainty analysis. Coast Eng 122:10–26. https://doi.org/10.1016/j.coastaleng.2017.01.008

Park H, Cox DT (2019) Effects of advection on predicting construction debris for vulnerability assessment under multi-hazard earthquake and tsunami. Coast Eng 153:103541. https://doi.org/10.1016/j.coastaleng.2019.103541

Petersen MD, Cramer CH, Frankel AD (2002) Simulations of seismic hazard for the Pacific Northwest of the United States from earthquakes associated with the Cascadia subduction zone. Pure Appl Geophys 159:2147–2168. https://doi.org/10.1007/s00024-002-8728-5

Pishief KS (2007) Community understanding and preparedness for tsunami risk in the eastern North Island, New Zealand. Unpublished MSc thesis, Department of Earth and Ocean Sciences, University of Waikato, Hamilton, New Zealand

Pidd M, de Silva FN, Eglese RW (1996) A simulation model for emergency evacuation. Eur J Opl Res 90(3):413–419. https://doi.org/10.1016/0377-2217(95)00112-3

Priest GR, Watzig RJ, Madin IP, Stimely L (2015) Local tsunami evacuation analysis of Seaside and Gearhart, Clatsop County, Oregon. Oregon Department of Geology and Mineral Industries Open-File Report O-15–02.

Priest GR, Stimely LL, Wood NJ, Madin IP, Watzig RJ (2016) Beat-the-wave evacuation mapping for tsunami hazards in Seaside, Oregon, USA. Nat Hazards 80:1031–1056. https://doi.org/10.1007/s11069-015-2011-4

Rahman MH (2018) Earthquakes don't kill, built environment does: evidence from cross-country data. Econ Model 70:458–468. https://doi.org/10.1016/j.econmod.2017.08.027

Remo JWF, Pinter N (2012) Hazus-MH earthquake modeling in the central USA. Nat Hazards 63(2):1055–1081. https://doi.org/10.1007/s11069-012-0206-5

Ritchie H, Roser M (2014) Natural disasters. Our World in Data. https://ourworldindata.org/natural-disasters. Accessed 20 Mar 2022

Rong Y, Jackson DD, Magistrale H, Goldfinger C (2014) Magnitude limits of subduction zone earthquakes. Bull Seismol Soc Am 104:2359–2377. https://doi.org/10.1785/0120130287

Rosenheim N, Guidotti R, Gardoni P, Peacock WG (2019) Integration of detailed household and housing unit characteristic data with critical infrastructure for post-hazard resilience modeling. Sustain Resilient Infrastruct 6(6):385–401. https://doi.org/10.1080/23789689.2019.1681821

Rosenheim N (2021) Detailed household and housing unit characteristics: data and replication code. DesignSafe-CI. https://doi.org/10.17603/ds2-jwf6-s535
Rozelle J (2018) International adaptation of the HAZUS earthquake model using global exposure datasets. Master's Thesis, University of Colorado at Denver.
Salazar K, Marcia KM (2011) Report on the 2010 Chilean Earthquake and tsunami response. Reston, Virginia: U.S Geological Survey
Sanderson D, Kameshwar S, Rosenheim N, Cox D (2021) Deaggregation of multi-hazard damages, losses, risks, and connectivity: an application to the joint seismic-tsunami hazard at Seaside. Oregon Nat Hazards 109(2):1821–1847. https://doi.org/10.1007/s11069-021-04900-9
Sanderson D, Cox D, Barbosa AR, Bolte J (2022a) Modeling regional and local resilience of infrastructure networks following disruptions from natural hazards. J Infrastruct Syst 28(3):04022021. https://doi.org/10.1061/(ASCE)IS.1943-555X.0000694
Sanderson DR, Cox DT, Amini M, Barbosa AR (2022b) Coupled urban change and natural hazard consequence model for community resilience planning. Earth's Future 10:e2022EF003059. https://doi.org/10.1029/2022EF003059
Shapira S, Levi T, Bar-Dayan Y, Aharonson-Daniel L (2018) The impact of behavior on the risk of injury and death during an earthquake: a simulation-based study. Nat Hazards 91:1059–1074. https://doi.org/10.1007/s11069-018-3167-5
Shuto N, Fujima K (2009) A short history of tsunami research and countermeasures in Japan. Proc Jpn Acad Ser B 85:267–275
Spence R, So E, Scawthorn C (2011) Human casualties in earthquakes: progress in modelling and mitigation. Springer, Berlin, p 322
Sugimoto T, Murakami H, Yozuki K, Nishikawa K, Shimada T (2003) A human damage prediction method for tsunami disasters incorporating evacuation activities. Nat Hazards 29(3):585–600. https://doi.org/10.1023/A:1024779724065
Suppasri A, Shuto N, Imamura F, Koshimura S, Mas E, Yalciner AC (2013) Lessons learned from the 2011 Great East Japan tsunami: performance of tsunami countermeasures, coastal buildings, and tsunami evacuation in Japan. Pure Appl Geophys 170(6–8):993–1018
Takabatake T, Shibayama T, Esteban M, Ishii H, Hamano G (2017) Simulated tsunami evacuation behavior of local residents and visitors in Kamakura, Japan. Int J Disaster Risk Reduct 23:1–4. https://doi.org/10.1016/j.ijdrr.2017.04.003
Takabatake T, Shibayama T, Esteban M, Ishii H (2018) Advanced casualty estimation based on tsunami evacuation intended behavior: case study at Yuigahama Beach, Kamakura, Japan. Nat Hazards 92:1763–1788. https://doi.org/10.1007/s11069-018-3277-0
Titov VV, Moore CW, Greenslade DJM, Pattiaratchi C, Badal R, Synolakis CE, Kânoğlu U (2011) A new tool for inundation modeling: community modeling interface for tsunamis (ComMIT). Pure Appl Geophys 168(11):2121–2131. https://doi.org/10.1007/s00024-011-0292-4
TRB (2010) Highway Capacity Manual 2010. Transportation Research Board, National Research Council, Washington, DC
Urrutia J, Bautista L, Baccay E (2014) Mathematical models for estimating earthquake casualties and damage cost through regression analysis using matrices. J Phys Conf Ser 495:012024
US Census Bureau (2020) Table P1 Total Population by race. 2020 Census redistricting data (Public Law 94–171). Accessed 13 July 2022. https://data.census.gov/cedsci/table?g=1600000US4165950&tid=DECENNIALPL2010.P1
van de Lindt JW, Ellingwood BR, Cutler H, Gardoni P, Lee JS, Cox D, Peacock WG (2019) The structure of the Interconnected Networked Community Resilience Modeling Environment (IN-CORE). In: Proceedings of 2nd international conference on natural hazards & infrastructure 23–26. Athens, Greece: National Technical University of Athens
Venturato AJ (2005) A digital elevation model for seaside, Oregon: procedures, data sources and analyses. NOAA technical memorandum OAR PMEL-129, NTIS: PB2006 101562, NOAA/Pacific Marine Environmental Laboratory, Seattle: WA. https://repository.library.noaa.gov/view/noaa/11061
Wang H, Mostafizi A, Cramer LA, Cox D, Park H (2016) An agent-based model of a multimodal near-field tsunami evacuation: decision-making and life safety. Transp Res C Emerg Technol 64:86–100. https://doi.org/10.1016/j.trc.2015.11.010
Wang Z, Jia G (2021) A novel agent-based model for tsunami evacuation simulation and risk assessment. Nat Hazards 105:2045–2071. https://doi.org/10.1007/s11069-020-04389-8
Wiebe DM, Cox DT (2014) Application of fragility curves to estimate building damage and economic loss at a community scale: a case study of Seaside, Oregon. Nat Hazards 71:2043–2061. https://doi.org/10.1007/s11069-013-0995-1

Wijerathne ML, Melgar LA, Hori M, Ichimura T, Tanaka S (2013) HPC enhanced large urban area evacuation simulations with vision based autonomously navigating multi agents. Procedia Comput Sci 18:1515–1524. https://doi.org/10.1016/j.procs.2013.05.319

Wilson R, Miller K (2014) Tsunami emergency response playbooks and FASTER tsunami height calculation: background information and guidance for use. California Geological Survey Special Report 236.

Witter RC, Zhang Y, Wang K, Priest GR, Goldfinger C, Stimely LL, English JT, Ferro PA (2011) Simulating tsunami inundation at Bandon, Coos County, Oregon, using hypothetical Cascadia and Alaska earthquake scenarios. In: Oregon department of geology and mineral industries special paper, vol 43, p 57

Wojahn SF (1976) Personality differences of two communities on the northern Oregon coast. Master of Science, Department of Geography. Oregon State University

Wood N (2007) Variations in city exposure and sensitivity to tsunami hazards in Oregon Scientific Investigations Rep. 2007–5283, US Geological Survey, Washington, DC

Wood NJ, Burton CG, Cutter SL (2010) Community variations in social vulnerability to Cascadia-related tsunami in the U.S. Pacific Northwest. Nat Hazards 52:369–389. https://doi.org/10.1007/s11069-009-9376-1

Wood NJ, Schmidtlein MC (2012) Anisotropic path modeling to assess pedestrian-evacuation potential from Cascadia-related tsunamis in the us pacific northwest. Nat Hazards 62(2):275–300. https://doi.org/10.1007/s11069-011-9994-2

Wood NJ, Schmidtlein MC (2013) Community variations in population exposure to near-field tsunami hazards as a function of pedestrian travel time to safety. Nat Hazards 65:1603–1628. https://doi.org/10.1007/s11069-012-0434-8

Wood NJ, Ratliff J, Peters J, Shoaf K (2013) Population vulnerability and evacuation challenges in California for the SAFRR tsunami scenario. Report 2013–1170-I, US Geological Survey, Washington, DC

Wood NJ, Wilson R, Jones J, Peters J, MacMullan E, Krebs T, Shoaf K, Miller K (2017) Community disruptions and business costs for distant tsunami evacuations using maximum versus scenario-based zones. Nat Hazards 86:619–643. https://doi.org/10.1007/s11069-016-2709-y

Wood N, Henry K, Peters J (2020a) Influence of demand and capacity in transportation simulations of short-notice, distant-tsunami evacuations. Transp Res Interdiscip Perspect 7:100211. https://doi.org/10.1016/j.trip.2020.100211

Wood N, Peters J, Wilson R, Sherba J, Henry K (2020b) Variations in community evacuation potential related to average return periods in probabilistic tsunami hazard analysis. Int J Disaster Risk Reduct 50:101871. https://doi.org/10.1016/j.ijdrr.2020.101871

Xie M, Murata M, Muraki Y (2017) Tsunami evacuation guidance simulation using multi-agent systems based on OpenStreetMap. Int J Environ Sci 2:231–237

Zhu R, Lin J, Becerik-Gerber B, Li N (2020) Human-building-emergency interactions and their impact on emergency response performance: a review of the state of the art. Saf Sci 127:104691. https://doi.org/10.1016/j.ssci.2020.104691

Zuccaro G, Cacace F (2011) Seismic casualty evaluation: the Italian model, an application to the L'Aquila 2009 event. In: Human Casualties in Earthquakes: progress in modelling and mitigation, pp 171–184

Authors and Affiliations

Mehrshad Amini[1] · Dylan R. Sanderson[1] · Daniel T. Cox[1] · Andre R. Barbosa[1] · Nathanael Rosenheim[2]

Daniel T. Cox
Dan.Cox@oregonstate.edu

Nathanael Rosenheim
nrosenheim@arch.tamu.edu

[1] School of Civil and Construction Engineering, Oregon State University, Corvallis, OR, USA

[2] Hazard Reduction and Recovery Center, College of Architecture, Texas A&M University, College Station, TX, USA